

Seismic Retrofit of Multi-Story RC Buildings by Encasement Technique

Almotasim B. J. F. Elabeidy

Submitted to the
Institute of Graduate Studies and Research
in partial fulfillment of the requirements for the degree of

Master of Science
in
Civil Engineering

Eastern Mediterranean University
February 2022
Gazimağusa, North Cyprus

Approval of the Institute of Graduate Studies and Research

Prof. Dr. Ali Hakan Ulusoy
Director

I certify that this thesis satisfies all the requirements as a thesis for the degree of Master of Science in Civil Engineering.

Prof. Dr. Umut Turker
Chair, Department of Civil Engineering

We certify that we have read this thesis and that in our opinion it is fully adequate in scope and quality as a thesis for the degree of Master of Science in Civil Engineering.

Prof. Dr. Mahmood Hosseini
Supervisor

Examining Committee

1. Prof. Dr. Mahmood Hosseini

2. Assoc. Prof. Dr. Umut Yildirim

3. Asst. Prof. Dr. Mohammad R. Bagerzadeh Karimi

ABSTRACT

Existing reinforced concrete buildings designed either considering gravity-only loads or following outdated provisions are deemed seismically deficient, especially if they are built in a seismogenic region. Consequently, many researchers have studied the possibility of strengthening these seismically weak structures to enhance their performance and mitigate losses in the event of intense seismic activity. However, most of the available retrofitting techniques in practice hinder the functionality of the vulnerable building and interrupt the inner workings during the upgrading process.

Therefore, this research proposes an efficient nondisruptive seismic retrofitting technique to externally strengthen seismically deficient reinforced concrete moment frame structures. The primary goal of this research was to develop a strategy where the entire retrofitting process is completed outside the building. The proposed encasement technique comprises a rigid peripheral framing system that confines the existing structure under seismic excitation to increase the stiffness and enhance the global seismic behavior.

The efficiency of the new system was verified by an exhaustive nonlinear three-dimensional dynamic simulation of selected multi-story reinforced structures, which was conducted using CSI ETABS. A performance-based assessment showed the capability of this system to rehabilitate existing weak structures as it showed an improved and satisfactory performance, notably in the case of low-rise buildings.

Keywords: reinforced concrete, seismic retrofitting, encasement technique, peripheral frames, nonlinear time history analysis, performance-based analysis.

ÖZ

Yalnızca yerçekimi yükleri dikkate alınarak veya eski hükümlere göre tasarlanan mevcut betonarme binalar, özellikle sismojenik bir bölgede inşa edilmişlerse, sismik olarak yetersiz kabul edilir. Sonuç olarak, birçok araştırmacı, yoğun sismik aktivite durumunda performanslarını artırmak ve kayıpları azaltmak için sismik olarak zayıf bu yapıların güçlendirilmesi olasılığını araştırdı. Bununla birlikte, uygulamada mevcut güçlendirme tekniklerinin çoğu, hassas binanın işlevselliğini engellemekte ve yükseltme işlemi sırasında iç çalışmaları kesintiye uğratmaktadır.

Bu nedenle, bu araştırma, sismik açıdan yetersiz betonarme moment çerçeve yapılarını harici olarak güçlendirmek için etkili bir yıkıcı olmayan sismik güçlendirme tekniği önermektedir. Bu araştırmanın birincil amacı, tüm güçlendirme sürecinin binanın dışında tamamlandığı bir strateji geliştirmektir. Önerilen kaplama tekniği, rijitliği artırmak ve küresel sismik davranışı geliştirmek için mevcut yapıyı sismik uyarma altında sınırlayan rijit bir çevresel çerçeveleme sistemini içerir.

Yeni sistemin verimliliği, CSI ETABS kullanılarak gerçekleştirilen, seçilmiş çok katlı güçlendirilmiş yapıların kapsamlı bir doğrusal olmayan üç boyutlu dinamik simülasyonu ile doğrulandı. Performansa dayalı bir değerlendirme, bu sistemin, özellikle düşük katlı binalarda, iyileştirilmiş ve tatmin edici bir performans gösterdiğinden, mevcut zayıf yapıları iyileştirme kabiliyetini göstermiştir.

Anahtar Kelimeler: betonarme, sismik güçlendirme, kaplama tekniği, çevresel çerçeveler, doğrusal olmayan zaman alanı analizi, performansa dayalı analiz.

ACKNOWLEDGMENT

First and foremost, I would like to praise Allah Almighty, the source of inspiration in my life and the one who blessed me with the strength without which I would not have completed this thesis.

I want to express my heartfelt gratitude to my thesis supervisor Professor Mahmood Hosseini for his guidance, support, and continuous encouragement thorough my study.

I am also sincerely thankful for the valuable friendships and fruitful discussions I had with my fellow postgraduates in the civil engineering department.

Finally, a special thanks to my family for their love and support. I am forever indebted to them for providing everything I needed throughout my endeavors.

TABLE OF CONTENTS

ABSTRACT	iii
ÖZ	iv
ACKNOWLEDGMENT	v
LIST OF TABLES	ix
LIST OF ABBREVIATIONS	xiii
1 INTRODUCTION.....	1
1.1 Overview and Current State of The Problem	1
1.2 Aim of The Study	2
2 LITERATURE REVIEW	3
2.1 Introduction	3
2.2 Performance Levels.....	3
2.3 Performance Objectives	5
2.4 Seismic Hazard.....	6
2.5 Deficiencies of The Existing MFRC Structures.....	7
2.5.1 Global Strength.....	8
2.5.2 Global Stiffness	8
2.5.3 Ductility	8
2.5.4 Configuration Irregularities	9
2.5.5 Continuous Load Path	10
2.5.6 Deterioration of Materials	10
2.6 Evaluation Procedures	10
2.6.1 Linear-Elastic Procedures.....	11
2.6.2 Nonlinear Static Procedure.....	11

2.6.3 Nonlinear Dynamic Procedure	12
2.7 Retrofitting Strategies	13
2.7.1 Member-Based Retrofitting	13
2.7.1.1 RC Column Jacketing	13
2.7.1.2 Beam-Column Joint Improvement.....	14
2.7.2 System-Based Retrofitting.....	15
2.7.2.1 Seismic Demand Control Strategies	15
2.7.2.1.1 Damping and Energy Dissipators	16
2.7.2.1.2 Base Isolation	16
2.7.2.2 Deformation Control Strategies	17
2.7.2.2.1 Steel Bracing.....	17
2.7.2.2.2 Shear Walls.....	20
2.7.2.2.3 External Frames.....	20
3 METHODOLOGY.....	23
3.1 Introduction	23
3.2 Research Strategy	23
3.3 General Plan Geometry and Gravity Load Assumptions	25
3.3 Materials Definition	27
3.4 Seismic Hazard and Seismicity Parameters	28
3.4.1 Assumed Site Class	28
3.4.2 Reference Peak Ground Acceleration.....	29
3.4.3 Seismic Actions	29
3.5 Ground Motion Records.....	31
3.6 Vulnerable Building's Cross-Sections	34
3.7 Proposed Retrofitting System.....	37

3.8 3D Modeling of The Buildings	38
3.9 Nonlinear Modeling	40
3.9.1 Concentrated Inelasticity Fiber Modeling	41
3.9.2 Calibration of The Gap Elements	44
4 RESULTS AND DISCUSSIONS	46
4.1 Introduction	46
4.2 Seismic Vulnerability Investigation	46
4.3 The Proposed Retrofitting System	49
4.4 Seismic Behavior of structures.....	53
4.4.1 Global Responses	53
4.4.1.1 Fundamental Periods.....	53
4.4.1.2 Roof Displacement.....	54
4.4.1.2 Roof Acceleration	60
4.4.1.2 Interstory Drift Ratio.....	65
4.4.1.2 Energy Components.....	72
4.4.2 Local Responses	74
4.5 Added Weight	80
5 CONCLUSION AND RECOMMENDATION	81
5.1 Conclusion.....	81
5.2 Recommendations	83
REFERENCES.....	85

LIST OF TABLES

Table 1: Load combinations.....	27
Table 2: Material properties.....	28
Table 3: General information for the chosen ground motion records.....	32
Table 4: Columns and beams cross-section of the considered vulnerable buildings.	35
Table 5: Optimized column cross-sections for the proposed retrofitting system	50
Table 6: Fundamental periods of structures.....	53
Table 7: Maximum roof displacements for 3-story structures.....	58
Table 8: Maximum roof displacements for 5-story structures.....	59
Table 9: Maximum roof displacements for 7-story structures.....	59
Table 10: Maximum roof acceleration for 3-story structures	61
Table 11: Maximum roof acceleration for 5-story structures	61
Table 12: Maximum roof acceleration for 7-story structures	62
Table 13: State of hinges in 3-story models.....	78
Table 14: State of hinges in 5-story models.....	79
Table 15: State of hinges in 7-story models.....	79
Table 16: Weight of structural elements for both vulnerable and retrofitted structures	80

LIST OF FIGURES

Figure 1: Illustration of the limit states as per EC8	5
Figure 2: The proposed retrofitting technique. (Elbahy et al., 2019)	15
Figure 3: The scaled lateral load resisting frame specimen and the design loads. (Youssef et al., 2007)	19
Figure 4: external retrofitting RC braced frame (Cao et al., 2020).....	21
Figure 5:Schematic diagram of the retrofitting mechanism of the SC-PBSPC braced frame (Cao et al., 2019).....	22
Figure 6: Followed approach in incorporating the adopted encasement technique ...	25
Figure 7: General beam and columns layout	27
Figure 8: Elastic and design response spectrum	31
Figure 9: Records frequencies and accelerations	33
Figure 10: Mean spectral acceleration spectrum for the scaled ground motion records	34
Figure 11: Idealized schematic view of the proposed retrofitting system	38
Figure 12: A sample of the Stress-strain relationship curves used in the analysis of the of the 3-story building. (a) Stress-strain curve of the confined concrete used for the columns, (b) the Stress-strain curve for the reinforcement, (c) the Stress-strain curve	41
Figure 13: Illustration of a typical fiber-type modeling for reinforced-concrete moment- frames. (NIST, 2017).....	43
Figure 14: Discretization of Fibers in Beams and Columns	43
Figure 15: The force-deformation relationship in gap elements	45

Figure 16: Linear analysis Demand/Capacity checks for column PMM ratio in the 3-story bare structure.....	47
Figure 17: Deficiencies identified by the linear analysis of the 5-story bare structure	48
Figure 18: Deficiencies identified by the linear analysis of the 7-story bare structure	49
Figure 19: 3D models of the proposed retrofitted structures and their section view .	52
Figure 20: 3-story buildings' roof displacement time history in response to "Imperial Valley-06" earthquake record	56
Figure 21: 5-story buildings' roof displacement time history in response to "Imperial Valley-02" earthquake record	57
Figure 22: 7-story buildings' roof displacement time history in response to "Imperial Valley-02" earthquake record	58
Figure 23: 3-story buildings' roof acceleration time history in response to "Imperial Valley-02" earthquake record	63
Figure 24: 5-story buildings' roof acceleration time history in response to "Imperial Valley-02" earthquake record	64
Figure 25: 7-story buildings' roof acceleration time history in response to "Imperial Valley-02" earthquake record	65
Figure 26: Interstory drift ratio for the 3-story models.....	67
Figure 27: Interstory drift ratio for the 3-story models (continued).....	68
Figure 28: Interstory drift ratio for the 5-story models	69
Figure 29: Interstory drift ratio for the 5-story models (continued).....	70
Figure 30: Interstory drift ratio for the 7-story models	71
Figure 31: Interstory drift ratio for the 7-story models (continued).....	72

Figure 32: The total energy components encountered by the 3-story models under “Superstition Hills-02” seismic activity.....	73
Figure 33: The total energy components encountered by the 5-story models under “Superstition Hills-02” seismic activity.....	74
Figure 34: The total energy components encountered by the 7-story models under “Superstition Hills-02” seismic activity.....	74
Figure 35: Hinge state at the end of Superstition hills 02 record for the 3-story models	76
Figure 36: Hinge state at the end of Superstition hills 02 record for the 5-story models	77
Figure 37: Hinge state at the end of Superstition hills 02 record for the 7-story models	78

LIST OF ABBREVIATIONS

ABRB	Assembled Buckling-Restrained Braces
ACI	American Concrete Institute
ASCE	American society of civil engineers
BRBF	Buckling-Restrained-Brace-Frame
CP	Collapse Prevention
CSI	Computers and Structures, Inc.
DCM	Medium Ductile Structures
DL	Damage Limitation
DL	Dead Load
EC	Eurocode
ETABS	Extended Three-Dimensional Analysis of Building Systems
FEMA	Federal Emergency Management Agency
IDR	Inter-Story Drift Ratio
IO	Immediate Occupancy
LFMA	Lateral Force Method of Analysis
LL	Live Load
LS	Life Safety
MFRC	Moment frame reinforced concrete structures
MRSA	Modal Response Spectrum Analysis
NC	Near Collapse
NEHRP	National Earthquake Hazards Reduction Program
NIST	National Institute of Standards and Technology
NTHA	Nonlinear-dynamic Time-History Analysis

PBSPC	Precast Bolt-Connected Steel-Plate Reinforced Concrete
PEER	Pacific Earthquake Engineering Research Center
PBD	Performance-Based Design
PGA	Peak Ground Acceleration
RC	Reinforced Concrete
SD	Significant Damage
SSMA	Superplastic Shape Memory Alloys

Chapter 1

INTRODUCTION

1.1 Overview and Current State of The Problem

Existing moment frame reinforced concrete structures (MFRC) built in the era prior to the enactment of modern seismic codes are mostly considered seismically vulnerable due to their limited ductility. In the event of strong ground motions, these buildings pose a significant risk to the life safety and economic wellbeing of societies since the buildings prone to damage include residential, commercial, and other critical facilities such as hospitals. The creation of such structural weaknesses could be attributed to several factors, with the most concerning being the prescriptive code design approach where the simpler linear static method is often adopted in seismic design. However, the inadequacies in this elastic design approach led to the development of a more viable and comprehensive Performance-Based Design (PBD) method to design and assess the response of buildings, particularly in seismogenic areas. This method is based on the premise that the structure's ability to survive an earthquake is essentially a function of its inherent inelasticity (nonlinear behavior) and deformation capacity rather than the initial yield strength (linear elastic behavior). In other words, ductile design and detailing requirements are the major focus in the newer codes to better mitigate seismic demands and reduce vulnerabilities.

As a result, the rehabilitation of older reinforced concrete (RC) structures has been a topic of concern for civil engineers worldwide, and over the last few decades a lot of

work has been put into developing retrofitting techniques and strategies as a mean to control lateral deformations and improve seismic capacity of these existing structures. An effective seismic risk mitigation begins with vulnerability assessment so that seismic retrofit techniques can be implemented appropriately. The addition of RC elements to improve the overall stiffness of the structure is one of the retrofit techniques implemented to strengthen seismically weak existing multi-story buildings, and a unique form of encasement technique forms the topic of this research and investigation.

1.2 Aim of The Study

This study aims to introduce encasement technique as a method for strengthening seismically deficient existing multi-story MFRC buildings. The application of this technique to the vulnerable buildings will be carried out through a computer-based finite element simulation. The buildings will be modeled using structural analysis software (ETABS) which will be further investigated and analyzed linearly utilizing the equivalent lateral force method, and nonlinearly using the nonlinear response time history dynamic analysis method. The earthquake effects as well as the performance after retrofitting is observed as compared to the original RC frames, and the efficiency of the proposed encasement technique will be evaluated through a performance-based approach.

Chapter 2

LITERATURE REVIEW

2.1 Introduction

In this chapter, the key concepts of seismic design and evaluation of buildings as per Performance-based philosophy are discussed, emphasizing the Eurocode guidelines and provisions which are adopted in this study as the reference standards. After defining the potential seismic hazards, performance levels, and objectives, this chapter thoroughly explains the weaknesses and deficiencies developed in reinforced concrete moment frames and how they affect the overall performance of the structure. Furthermore, different evaluation procedures and analysis methods used to assess existing structures are presented. Finally, an extensive literature review has been conducted to showcase the most commonly used retrofitting techniques and strategies, ordered to be in line with the scope of this research and to justify the choice of the method later on.

2.2 Performance Levels

In the modern era, the performance based is the predominant approach to evaluate seismic design and structural retrofitting. The performance-based approach involves, the behavior of the building as a whole which depends on the interaction of its individual elements, including the main load-carrying components as well as the non-structural components. The most common seismic standards and retrofitting documents such as Eurocode 8: Design of structures for earthquake resistance (EC8), seismic rehabilitation of existing building (ASCE 41–06), Prestandard and

commentary for the seismic rehabilitation of buildings (FEMA 356) or NEHRP guidelines for the seismic rehabilitation of buildings (FEMA 273) classifies the seismic performance of a building into several levels depending on the impact of earthquakes and the damage state of the building components, which can be described by displacements, strains, rotations, or even changes in the energy dissipating mechanism of the structure.

In this study, EC8 is adopted as the primary guideline for seismic design and evaluation of the modeled structures. This section primarily focuses on the performance levels and limit states defined in Eurocodes, which are characterized as follows:

- **Near Collapse (NC):** The structure is damaged heavily while the non-structural elements are entirely collapsed due to the enormous lateral drifts. In this case, the structure only attains minimal residual strength and stiffness in all stories, which hinders its ability to survive another earthquake, even of moderate intensity, despite that it might still be capable of sustaining gravity loads. NC corresponds to the Collapse Prevention (CP) performance level used in ASCE 41–06.
- **Significant Damage (SD):** The structure is damaged significantly with moderate permanent drifts. However, the structure has some residual lateral strength and stiffness, and only vertical loads are sustained by the columns. Non-structural components are also damaged, although no out-of-plane failures are present in partitions and infill. At this level, the structure is capable of sustaining after-shocks of moderate intensity. In ASCE 41–06, this type of performance is called Life Safety (LS).

- **Damage Limitation (DL):** The structure is only damaged lightly, without significant yielding of the structural element, and the overall strength and stiffness properties are preserved. In addition, only minor cracks are developed in non-structural elements. In this case, the damage can be economically repaired and overall, the structure does not need retrofiting. ASCE 41–06 refers to the same limit state as Immediate Occupancy (IO) performance level.

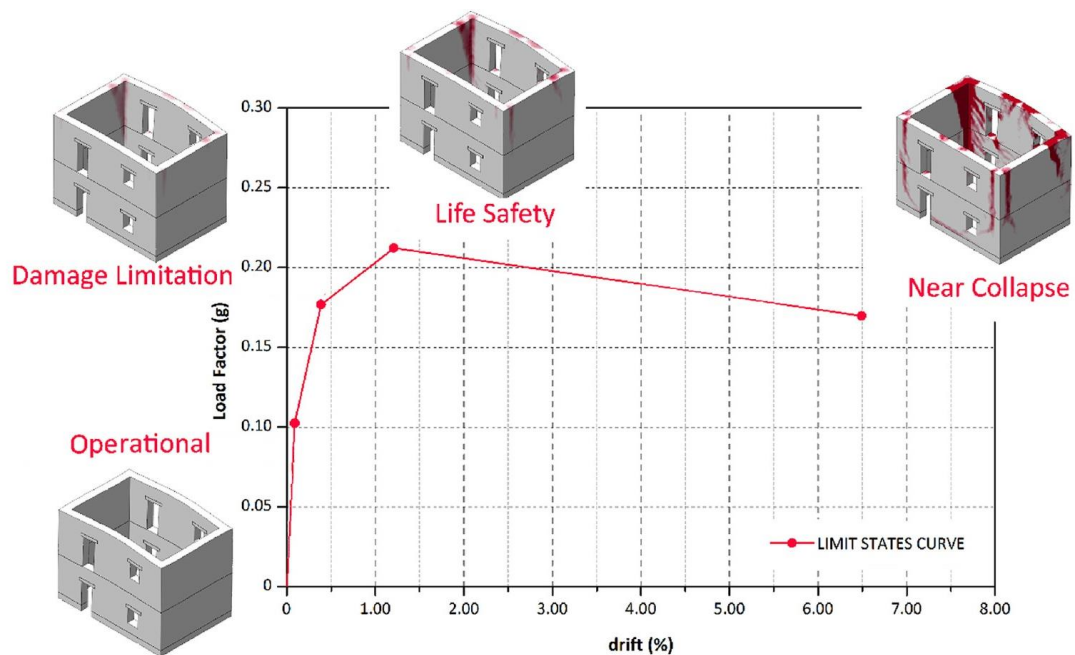


Figure 1: Illustration of the limit states as per EC8

A point to be noted that, FEMA 356 (2000) provides a more detailed description of the performance levels of buildings since it also specifies the seismic performance levels for each individual component within the structure.

2.3 Performance Objectives

The idea behind the seismic design is not simply producing an earthquake-proof structures which does not be damaged even under extreme, but infrequent, ground motions; this design philosophy often produces unnecessarily too robust and expensive

buildings. Instead, the engineering intention of the current seismic design codes is to construct ductile buildings that may get damaged however without jeopardizing the safety of human life. The level of damaged allowed depends on the functionality of the building. For instance, emergency services and stations that have a vital role in after-earthquake management have to maintain its functionality immediately upon the end of ground motion and the aftershocks; therefore, such structures must endure limited damage and should provide a greater level of protection against earthquakes. By taking into account the aforementioned definitions, the design philosophy can be outlined as:

- In the event of weak frequent seismic action, the structural components should remain within the elastic range; however, the non-structural elements may undergo some repairable damage.
- In the event of occasional ground shaking of moderate-intensity, the structural components may sustain some repairable damage, while non-structural elements may be damaged severely.
- In the event of rare strong ground shaking, the structural components may sustain severe damage, but without exceeding the NC limit state.

Therefore, a successful seismic design must meet the desired performance objectives by controlling the damage at a reasonable cost. These objectives are selected based on the structure's functionality and category, and the of the earthquake intensity (Ambrose & Vergun, 1999).

2.4 Seismic Hazard

To meet the objectives of a seismic design, representative earthquake ground motions for the potential seismic hazards have to be determined taking into account previously

formed faults and tectonic activities, the behavior of seismic waves traveling through the soil medium, and the near-surface site conditions at the location of interest. There are two basic ways to express seismic hazards such as the deterministic and the probabilistic seismic hazard analysis approach. In the deterministic approach, the maximum expected earthquake occurring at the nearest distance from the location of interest is taken into account to estimate the ground motion parameters. However, deterministic approach does not consider the likelihood of exposure during the lifetime of the structure. Alternatively, the probabilistic approach incorporates all of the effects of the anticipated seismic activities occurring during a specified life span of the structure. Nevertheless, EC8 utilizes the latter approach by using seismic hazard maps or zones that describe the local hazards associated with earthquakes in a particular region. For most applications, in terms of a single seismological parameter, such as the reference peak ground acceleration (PGA) corresponding to a probability of exceedance in 50 years (P_{NCR}) for NC limit state requirement is utilized. In other words, this zoning-based technique uses maps of PGA with respect to a reference probability of exceedance to define seismic input at various hazard levels and under different site conditions.

2.5 Deficiencies of The Existing MFRC Structures

Deficiencies in a structural system occurs when the seismic demands produce unacceptable limit states, and the behavior of the structure does not meet the performance objective of the design. These deficiencies can be addressed by identified by a thorough evaluation of the global structural configuration, the lateral force-resisting system, the characteristics of the material used, and the reinforcement detailing of the elements. The dynamic response to a ground motion is governed by the overall strength, stiffness, ductility, and damping of the structural system. The

following is a brief description of the sources of deficiencies in MFRC structures in light of the aforementioned properties.

2.5.1 Global Strength

In MFRC structures, global strength commonly refers to columns' total lateral strength capacity provided at each story. Global strength deficiencies is typically found in old structures built before the 1970s, where the absence of capacity design philosophy as per current regulations is accentuated primarily because the main objective of the design was to provide strength only to sustain gravitational loads without considering lateral demands (Arlekar et al., 1997).

2.5.2 Global Stiffness

The stiffness of MFRC structures is developed mainly from the vertically oriented structural elements and the diaphragms that constitute the lateral force-resisting system. Stiffness is the core property in the dynamic behavior that dominates the modes of deformations and story drifts upon ground shaking. Moreover, the seismic forces experienced by the structure are distributed based on the distribution of stiffness and mass along its height which can be a major source of seismic deficiencies in a system (Hertanto, 2005).

2.5.3 Ductility

Ductility of structures can be defined as their ability to dissipate energy through a number of cycles of nonlinear deformation without substantial degradation of the load-bearing capacity, which is the paramount consideration in seismic design and assessment. Non-ductile MFRC structures are vulnerable to the undesired brittle failure mechanisms during an earthquake, experienced as the rapid drop in strength and stiffness of the structural components. The lack of ductility has been acknowledged as the fundamental source of seismic deficiencies in old RC buildings

(Pampanin et al., 2002). At the global level, material properties, loading mechanism (cyclic or monotonic), and column/beam capacity relationship dictate the ductility capacity of the structure, whereas, at the local level, element detailing is the key to achieving robustness through ductility, especially in beam-column joint connection and panel zones. Typically, ductile deficiencies are emphasized by Yakut, (2004) as follows:

- Lack of adequate confinement through transverse ties and stirrups due to large reinforcement spacing.
- Inadequate column lap splices for the longitudinal reinforcement, or if they are located in the potential plastic hinge area.
- Inadequate anchorage of beam reinforcement.
- Inadequate or even absence of beam-column joint transverse reinforcement.

2.5.4 Configuration Irregularities

As per EC8 guidelines, buildings are classified as regular or irregular structures. No considerable discontinuities in plan, vertical configuration or lateral force resisting systems are present in structures deemed regular. In such systems, the building experience less damage due to the uniformly distributed mass and stiffness in plan and elevation. In contrast, the non-uniform distribution of mass and stiffness along the building's height in irregular structural configurations cause stress concentrations and consequently higher seismic demands, resulting in an excessive occurrence of deformations. One of the main ramifications of irregularities in configuration is the formation of weak stories (a story that possesses a lower lateral structural strength than the immediate story above or the rest of the stories of the building) and soft stories (a story that possesses a lower lateral structural stiffness than the rest of the stories of the building) (Varadharajan et al., 2014).

2.5.5 Continuous Load Path

A safe load transfer mechanism is the most decisive requirement for the structural safety of buildings, which is directly linked with the regularity and irregularity of the structural anatomy. Under the application of seismically induced forces (earthquake inertial forces), it is mandatory to provide a continuous load path having enough stiffness and strength from the source of these forces to the soil through the rigid diaphragms, columns, and foundation system. Therefore, ensuring a continuous load path throughout the seismic excitation is paramount in terms of structural integrity and collapse prevention. This can be secured by providing sufficient redundancy in the system in case of element failure. (Basnet, 2021).

2.5.6 Deterioration of Materials

Deteriorated structural materials create undesirable subsidiary effects on the seismic performance of the existing building. For instance, cracks may develop in concrete due to spalling (exposure of concrete to extremely high temperatures), shrinkage (excessive drying of concrete during curing), or disintegration (exposure to contaminants such as contaminated aggregates, water, or cement). This can cause corrosion of steel reinforcement as a consequence of moisture penetration through the pathways developed from the cracks. Therefore, damage assessment must be evaluated based on the existing condition of the structure rather than the design parameters as the materials' current state significantly affects the structure's integrity and directly influences its performance under seismic forces.

2.6 Evaluation Procedures

Several analysis procedures are used to measure seismic demands, capacities, and performance of MFRC structures. These procedures are suitable for identifying structural deficiencies of an existing building or verifying the effectiveness of a

proposed retrofitting strategy. EC8 outlines three different evaluation procedures to assess the structural response under earthquake excitation: Linear elastic procedures, Nonlinear static procedure (i.e., push-over analysis), and Nonlinear dynamic procedure. The method of choice depends on the objectives of the analysis and the type of structure under investigation.

2.6.1 Linear-Elastic Procedures

In these procedures, the buildings are modeled on the basis of linear-elastic behavior of the structure utilizing the initial stiffness and equivalent viscous damping values on par with the approaching-yield response of components. EC8 suggests two types of linear analysis depending on the structural properties: the Lateral Force Method of analysis (LFMA) and Modal Response Spectrum analysis (MRSA). LFMA is recommended when the building is free of irregularities in elevation, and the fundamental first mode of vibration sufficiently represents the dynamic response. In comparison, MRSA is applicable to all types of buildings, and it is the standard method used in seismic design. When the linear procedures are used to calculate internal forces and the resulting drifts, the lateral force due to the seismic action is distributed over the height of the building according to the structure's weight and stiffness allocation. Although the design spectrum used in both incorporates the inelastic behavior through a behavior factor q that accounts for overstrength and ductility of the building, it is challenging to obtain precise results for structures that actually undergo nonlinear deformations using linear-elastic procedures. Thus, EC8 guidelines advise against the use of linear procedures while evaluating irregular structures.

2.6.2 Nonlinear Static Procedure

The nonlinear static method, collectively known as push-over analysis, is a performance-based method of analysis that evaluates the structural performance of

buildings by comparing the deformation capacities to the seismic demands at the desired performance level. While keeping constant gravity loads during the analysis, a monotonically increasing lateral load is applied at the location of the masses to trigger the inertia forces until a target drift is attained or a collapse is observed. The target drift is meant to represent the ultimate deformation the building is likely to experience during the seismic action. Push-over analysis is widely used in engineering practice because it can reasonably estimate the inelastic behavior and identify the failure mechanisms with minimal numerical complexity compared to the nonlinear dynamic procedure.

2.6.3 Nonlinear Dynamic Procedure

The nonlinear dynamic time-history analysis (NTHA), similar to push-over analysis, needs a mathematical model which takes into account post-yield behavior of the structural material. Nevertheless, instead of relying on target displacement values, the displacements and dynamic responses are obtained through direct numerical integration of the differential equations of motion. The seismic action in this method is represented by ground motion time-history accelerograms specific to the site of interest. NTHA is highly sensitive to the time-history records used to depict the seismic hazard; that is why EC8 requires a minimum of 3 records to be selected and scaled to express the ground motion adequately. The scaling is carried out such that the mean 5% damping elastic spectrum calculated from all the records in the range of periods between 20% and 200% of the fundamental period of the structure is greater than 90% of the corresponding value from the 5% damping elastic response spectrum. This type of analysis is often used in research studies because the nonlinear response is explicitly modeled, resulting in a more accurate dynamic response estimation. Nevertheless,

engineers are often deterred from using NTHA as it is time-consuming and requires powerful computational resources.

2.7 Retrofitting Strategies

The current strengthening methods are intended to address and improve some or all of the structural deficiencies listed above. These methods may basically be categorized into two main groups: Member-based retrofitting and System-based retrofitting (Moehle, 2000).

2.7.1 Member-Based Retrofitting

The aim of member-based retrofitting is to increase the strength or ductility of the structural members individually so that their limit states are not exceeded as the building responds to lateral loading. The main member-based strengthening techniques are centered around column jacketing and beam-column joint improvement. Such techniques increase the member's local ductility, enabling it to absorb more energy while sustaining a stable response at larger lateral deformation demands.

2.7.1.1 RC Column Jacketing

Reinforced concrete jacketing is considered one of the most commonly applied methods for local retrofitting and repairing of concrete structural elements. As the name suggests, this technique involves the encasement of the deficient element with a reinforced concrete jacket (i.e., layer) (Campione et al.,2014; Minafò, 2015). A proper bonding between the existing concrete and the RC jacket can be attained by roughening up the surface of the old concrete element or by applying certain adhesives on the interface between the jacket and the existing concrete (Ali 2009). RC jacketing provides a uniform increase in stiffness and ductility throughout the element, thereby improving the load-carrying capacity of the element while avoiding the possible

concentrations of lateral load resistance, which might occur in the case of the addition of shear walls for example. (Rodriguez & Park, 1991; Kaliyaperuma & Sengupta, 2009). In some cases, RC column jacketing can be deemed a system-based intervention technique if the longitudinal reinforcement in the jacket does not stop at the floor level and passes through the slab depth. In addition to being intrusive in nature as a retrofitting strategy, another drawback of RC jacketing is that the longitudinal reinforcement in the jacket often needs to be bundled at the corners of the added layer due to the presence of beams; on the other hand, it is challenging to provide transverse reinforcement (cross ties) for the longitudinal bars in the jacket if they are not bundled at the corners because of the presence of the weak structural member in the middle. Some recent studies suggested using fiber-reinforced polymer to overcome those disadvantages arising from using steel reinforcement in the jackets (Ilki et al., 2009).

2.7.1.2 Beam-Column Joint Improvement

The poor reinforcement detailing of the beam-column joints is a common source of deficiency in existing RC structures, resulting in brittle failure mechanisms. To overcome this, the ductility of the elements can be increased by utilizing smart materials such as Superplastic Shape memory Alloys (SSMA) at the joints. SSMA can be used internally as reinforcing bars or additional transverse reinforcement as they can withstand larger deformations than the typical steel reinforcement while maintaining the ability to return to their undeformed shape upon unloading. Also, they provide higher damping properties and good resistance against corrosion. Moreover, SSMA can be used externally at the beam-column joints to locally improve the seismic performance of vulnerable joints (Alam et al., 2009; Youssef & Elfeki, 2012). Elbahy et al. (2019) studied the effect of externally retrofitting weak MFRC structures with SSMA assembly placed at the critical joint locations, as shown in Figure 2. The study

showed that the retrofitted frames were able to tolerate higher earthquake intensities with less damage compared to the original RC frame. This proposed retrofitting technique decreased the maximum lateral drifts undergone by the frame by 10-15% and the residual deformation by 50-70% (Elbahy et al., 2019).

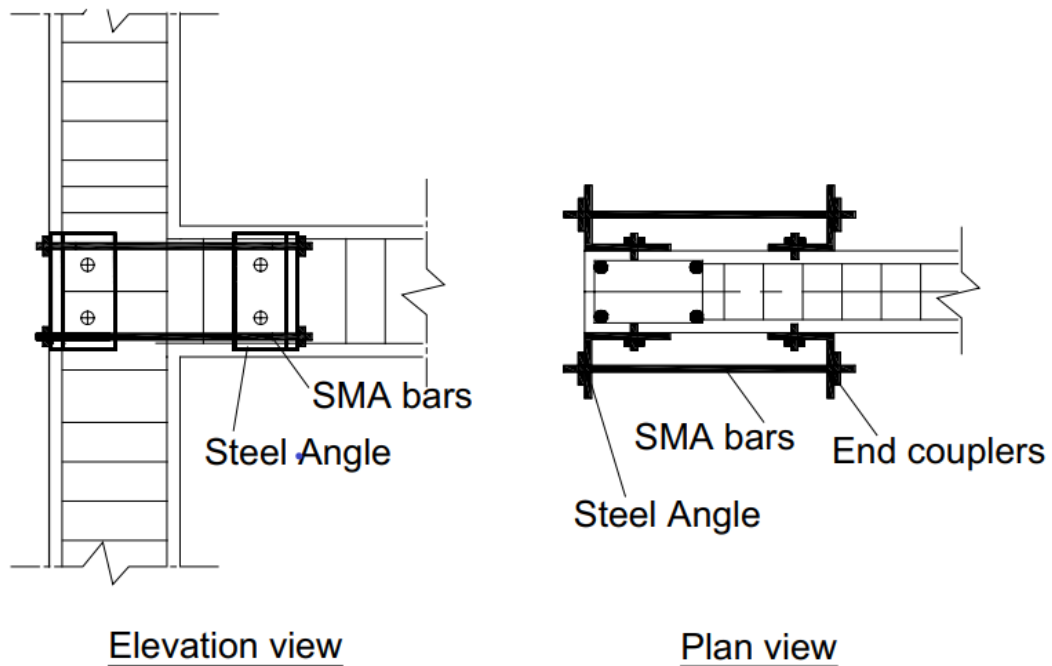


Figure 2: The proposed retrofitting technique. (Elbahy et al., 2019)

2.7.2 System-Based Retrofitting

In System-based retrofitting, the improvement in strength and dynamic behavior of the entire structure is achieved by the addition of new structural members to the existing system (Bouvier, 2003). The strengthening techniques used in this method are either based on reducing seismic demands, or controlling drifts and deformations by increasing the stiffness.

2.7.2.1 Seismic Demand Control Strategies

The retrofitting techniques under this category seek to improve the performance by reducing seismic force demands based on weight reduction, providing supplementary

dampers and other auxiliary energy dissipation sources, or seismic base isolation. However, it should be noted that the aforementioned weight reduction method is outdated as it is not a practical solution for most cases, especially if the functionality of the building cannot afford losing the space. Additionally, when the weight of the structure is reduced, the fundamental period decreases, which often leads to higher seismic demands; that is why this method of retrofitting has been highlighted as a major concern by many researchers in this field of study (Tena-Colunga et al., 1996; Giuseppe & Massimo, 2005).

2.7.2.1.1 Damping and Energy Dissipators

The effectiveness of dampers in seismic retrofitting has been proven both experimentally and in practice especially in the event of intense ground shaking (Cheung et al., 2000; Soong et al. 2002; Habibi et al., 2013). For vulnerable flexible systems, such as MFRC buildings, providing supplementary damping devices are usually more suitable compared to other strategies such as base isolation. Passive damping devices are the most common in this approach, including viscous fluid dampers and friction dampers. The main purpose of such devices is to decrease the non-linear energy dissipation demand on the structural frame. This can reduce the lateral damage and acceleration response by lowering the intensity of the shear forces distributed along the building's height (Constantinou & Symans, 1993; Symans et al., 2008). Although, damping systems have the advantage of being less intrusive, the high implementation costs are a major drawback in most cases.

2.7.2.1.2 Base Isolation

Base isolation is recognized as a very effective method to enhance the dynamic behavior of structures subjected to seismic action without interfering with global stiffness. In general, isolation devices are placed at the bottom of the ground floor

columns resulting in a prolonged fundamental period for the structure, which significantly reduces the transmission of acceleration from the ground to the superstructure above the isolation interface (Naeim & Kelly, 1999). This method of retrofitting is considered an intrusive technique since it requires intervention to connect all the bottom columns to the isolating devices. This can introduce a challenging problem to the engineers involved in the assessment and retrofitting since the superstructure above the base columns needs to be temporarily supported to install the isolation devices without endangering the structure's anatomy or creating deficiencies. For instance, extensive research done by the International Rubber Research and Development Board of the United Kingdom suggested that base isolation is not only functional as a safety measure in seismogenic regions but also cost-efficient (Chandrakar & Singh, 2017). Another study compared traditional and innovative seismic safety strategies and measures concluded that the use of base isolation as the lateral force-resisting system guarantees a higher degree of protection against seismic activity than what is provided by implementing energy dissipators, regardless of the type of devices employed (Bruno & Valente, 2002).

2.7.2.2 Deformation Control Strategies

Deformation control techniques mainly involve the integration of shear walls, bracing elements, or external frames to the existing structural configuration. However, the consequent increase in structural stiffness of the retrofitted system using these strategies should be thoroughly evaluated since the period of the structure may be reduced, hence attracting higher seismic forces.

2.7.2.2.1 Steel Bracing

The addition of bracing to a non-ductile RC structure is one of the most effective retrofitting strategies that have been in practice for the past 50 years. The braces, which

are typically made of steel, are added to the vulnerable system to improve the overall strength and stiffness, resulting in a decreased lateral drift. (Moehle, 2000). The advantages of using steel braces include the capacity to accommodate openings, the minimal additional weight, the distribution flexibility, and in the case of external bracing systems, most of the construction work will be performed outside of the building, limiting the disruption to the building operation. However, steel brace systems are often costly, especially when members are exposed to external weather conditions, which calls for maintenance on a regular basis (Bouvier, 2003).

There have been a number of studies on the effect of the retrofitting of non-ductile MFRC structures with steel bracing (Pincheira & Jirsa, 1995; Masri & Goel, 1996; Safarizk et al., 2013; Navya & Agarwal, 2016). Some selected experimental studies are introduced herein. Youssef et al. (2007) investigated the efficiency of incorporating a bracing system to RC frames to increase ductility and improve seismic performance. This study examined two scaled frames: one was designed and detailed as per the American Concrete Institute (ACI) 318 code, and the second frame had the proposed concentric slender double angle bracing elements integrated, as shown in figure 1. Both frames were 1/2.5 of the conventional four-story RC structure. For the ordinary frame, the researchers observed that nonlinear response initiated at the bottom reinforcement in of the bottom beam and consequently failure occurred at the ends of the beams. Moreover, only flexural cracks were developed in elements without any noticeable shear cracks. However, fewer cracks were observed in the steel braced frame, and the nonlinear behavior was initiated through the yielding of steel elements. Upon further loading, buckling of the steel occurred, followed by the development of plastic hinges at the ends of the beams, similar to the failure mechanism of the ordinary

frame. The results indicated that the bracing system increased the stiffness of the moment frame by 200%, and the lateral capacity was 256% greater. Nonetheless, the maximum drift experienced by the bare frame was 4.0%, whereas the retrofitted frame sustained a 5.0% drift ratio. Also, the energy dissipated by the braced frame was roughly twice that of the ordinary frame.

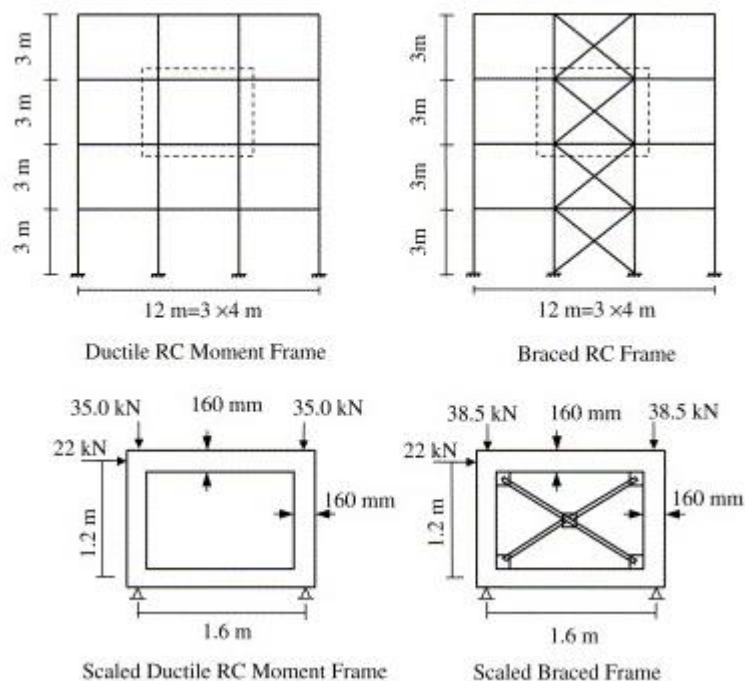


Figure 3: The scaled lateral load resisting frame specimen and the design loads. (Youssef et al., 2007)

Maheri and Ghaffarzadeh (2008) took the work of Youssef et al. (2007) a step further by introducing a different section for bracing. The study explored the interaction level between the RC frame's strength capacities and the bracing system. The new frame, referred to as FX2, was constructed with the same dimension as the bare moment frame and was braced by a non-slender steel channel cross-section. FX2 started yielding at 2.5% drift ratio and failed at 4.3% drift, compared to the respective 2.08% and 4.0% drifts experienced by the braced frame (FX1) in the Youssef et al. (2007) experiment.

According to the researchers, both braced frames FX1 and FX2 had greater capacities than the sum of the individual non-braced frame and the bare bracing capacities. The capacities of FX1 and FX2 increased by 8.5% and 7%, respectively, in comparison.

2.7.2.2.2 Shear Walls

One of the most common ways to strengthen seismically endangered structures is the addition of new RC walls systems. The added elements provide enough stiffness in the system to control the global lateral drift, which reduces the damage occurring in the structural members under lateral loading. The location of the added shear wall is of utmost importance as it influences the structure's deformation mode and might cause undesirable torsional demands. Moreover, the path of the transferred loads from the rigid diaphragm towards the foundations, as well as the possible stress concentrations, depends on the selected location, which calls for a careful evaluation (Kaplan et al., 2011). The placement location is also required to be strategically selected such that the wall will be bounded with the preexisting structural elements. On some occasions, shotcrete is used to enhance the bonding connection between the existing structural elements and the added shear wall. The design procedure for such shear walls is similar to that of a traditional shear wall in new structures; however, vigilance is needed to grant flexural ductility by providing well confinement. Another critical factor in the design is to ensure that enough capacity to resist the high shear loads is developed within the elastic limits without the susceptibility of brittle failure (Frosch et al., 1996).

2.7.2.2.3 External Frames

Since the 1970s, researchers worldwide have studied the possibility of externally upgrading the seismically weak structure to mitigate the structural response and enhance the performance of the structure as a whole. The primary goal was to develop retrofitting strategies that do not require interrupting the inner workings with the entire

upgrading process being completed outside the building. To date, external strengthening techniques have concentrated on system-based structural retrofitting, featuring distinctive forms such as the external moment frames or braced frames. With the considerable increase in lateral stiffness and the ease of connection to the existing building, RC braced frames, as shown in Figure 3, have been the most commonly used in practice (Cao et al., 2020). Nonetheless, many studies have indicated that the primary failure mechanism of the external braced frames due to ground shaking is the out-of-plane buckling of braces. This received widespread attention and led to the development of Assembled Buckling-Restrained Braces (ABRB) as an alternative to the steel bracing typically used. ABRB delivered superior mechanical properties under compressive stresses and provided the choice of replacing the damaged plates after failure (Usami et al., 2012; Iwata & Murai, 2006; Dusicka & Tinker 2013). Despite the studies that proved the immaculate energy-dissipation capacities of such elements, the applications of this type of braced frames in seismic retrofitting might yield immense residual deformations, demanding costly repairs following a seismic event. Moreover, most of the aforementioned experimental studies were conducted in comparison to bare frames without infills and facades; however, in real cases, these components cannot be overlooked, which may leave no room for the addition of braces (Xie, 2005).

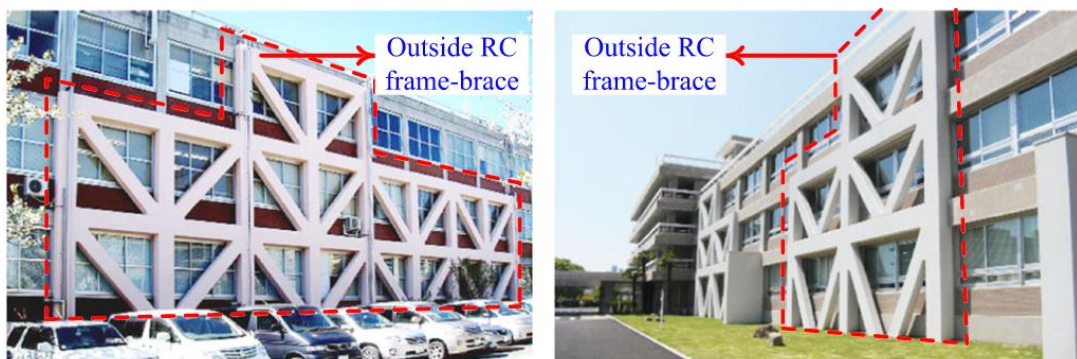


Figure 4: external retrofitting RC braced frame (Cao et al., 2020)

Cao et al. (2020) proposed an innovative external retrofitting method (Figure 5) that employs self-centering precast bolt-connected steel-plate reinforced concrete buckling-restrained-brace-frame (PBSPC BRBF). This method combines the energy dissipation capacity of the ABRB with the ample displacement control of the prestressed tendons and precast assembly to acquire the ideal lateral force resisting capacity. The combination of these technologies together with the existing MFRC boosts the overall structural performance of the integrated system as a global or system-based retrofit in terms of residual deformations and stiffness characteristics.

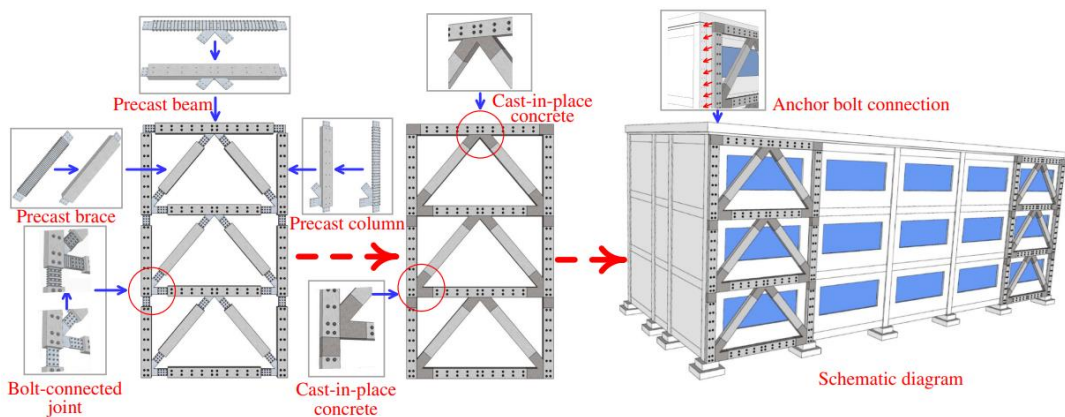


Figure 5: Schematic diagram of the retrofitting mechanism of the SC-PBSPC braced frame (Cao et al., 2019)

Chapter 3

METHODOLOGY

3.1 Introduction

This chapter is intended to describe the general research strategy followed to evaluate the proposed retrofitting technique's performance compared to the bare benchmark structures. To start with, a detailed flowchart summarizing the research methodology is presented. After that, the adopted plan geometry of the studied structures and elements' sections will be detailed. Moreover, the seismicity parameters used in the design and evaluation as per the Eurocodes are discussed together with the selected earthquake records. Finally, the procedure followed for both linear and nonlinear modeling will be explained in a comprehensive manner.

3.2 Research Strategy

The primary objective of this study is to investigate the effectiveness of a proposed non-destructive retrofitting technique as a method for enhancing the seismic capabilities of existing vulnerable RC moment frame structures. To accomplish this, a research methodology has been designed as shown in Figure 6. As the number of stories highly influences the seismic behavior of structures, three multistory RC moment frame structures having the same geometrical plan, but differ in the number of stories, are selected as the study's benchmark. These buildings are designed under the actions of gravity and seismic loads as per the Eurocodes. The preliminary design is conducted utilizing materials of high strength and after assessing the adequate sections for the beams and columns, the material properties are downgraded such that

deficiencies are created within the structural system leaving the building seismically weak and vulnerable to collapse under earthquake excitation. These vulnerable structures are subjected to nonlinear time history to assess their actual nonlinear response under seismic actions. Then the weak structures are retrofitted with the proposed peripheral rigid frame; this is followed by conducting a series of iterations of nonlinear time history analysis to optimize the cross-section of the introduced external frames. At the end of each iteration, the rigidity of the external frames is adjusted until the building's seismic performance surpasses the desired limit state category.

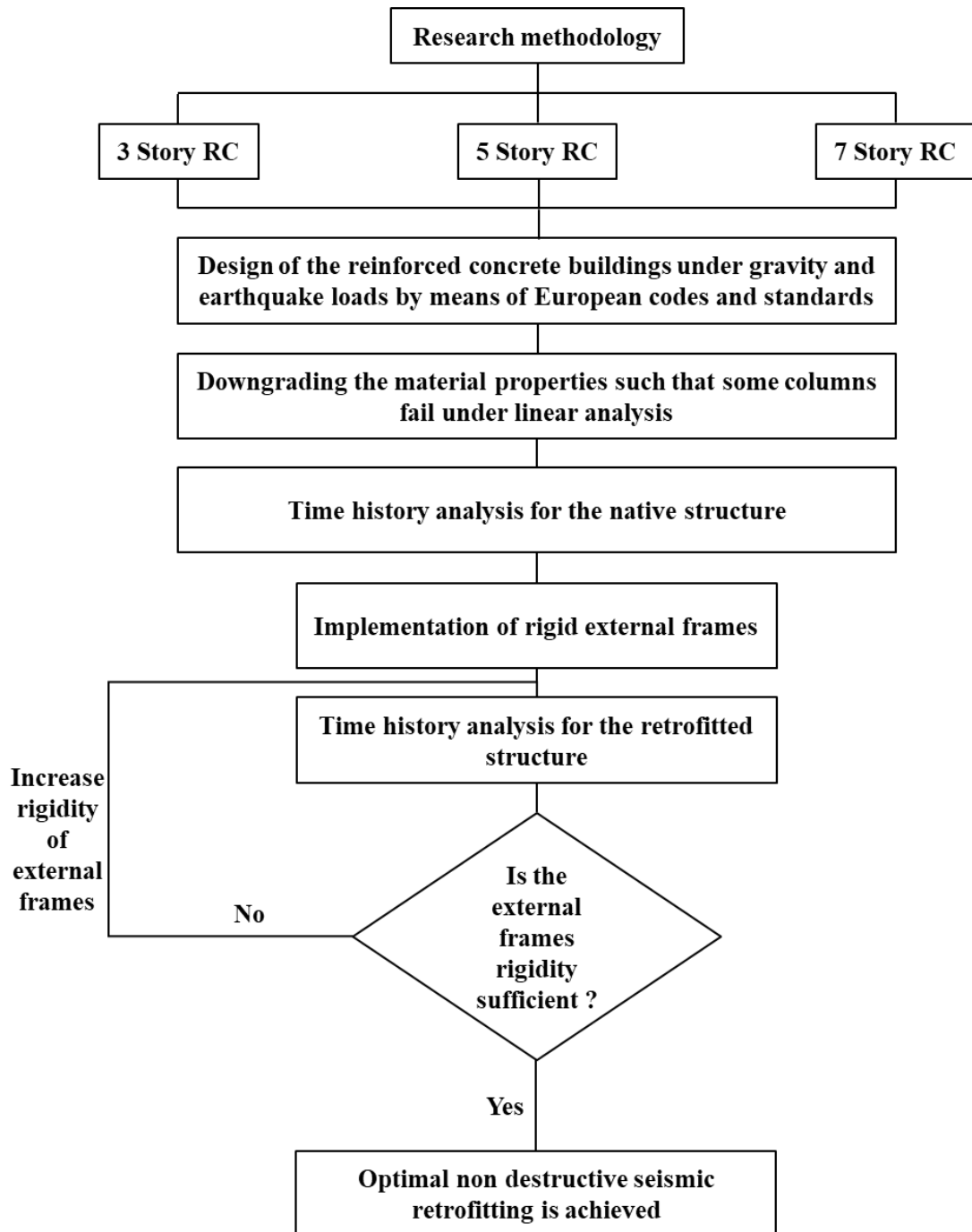


Figure 6: Followed approach in incorporating the adopted encasement technique

3.3 General Plan Geometry and Gravity Load Assumptions

The general plan geometry of the reinforced concrete building studied is illustrated in Figure 7. As shown, the plan is composed of rigid moment frames spanning three bays

in both perpendicular directions. The spacing between columns is 5 meters, center to center, and all stories are 3 meters in height.

In addition to the self-weight of the structural elements, uniformly distributed imposed and dead loads acting on all floors were taken into account both in the linear design and the nonlinear analysis. The dead load amounted to 2 kN/m^2 after considering the finishing and screed at each floor, while the roof super-dead load was added up to be 1.5 kN/m^2 . Similarly, the imposed live loads were taken from the prescribed loads for the residential buildings category in the Eurocodes; that is 2 kN/m^2 for the typical floor and 1.5 kN/m^2 for the roofs. Furthermore, the wall load was applied on the external beams as uniformly distributed 5 kN per unit meter, assuming light clay brick is used. Table 1 shows the load combination used for the linear elastic design.

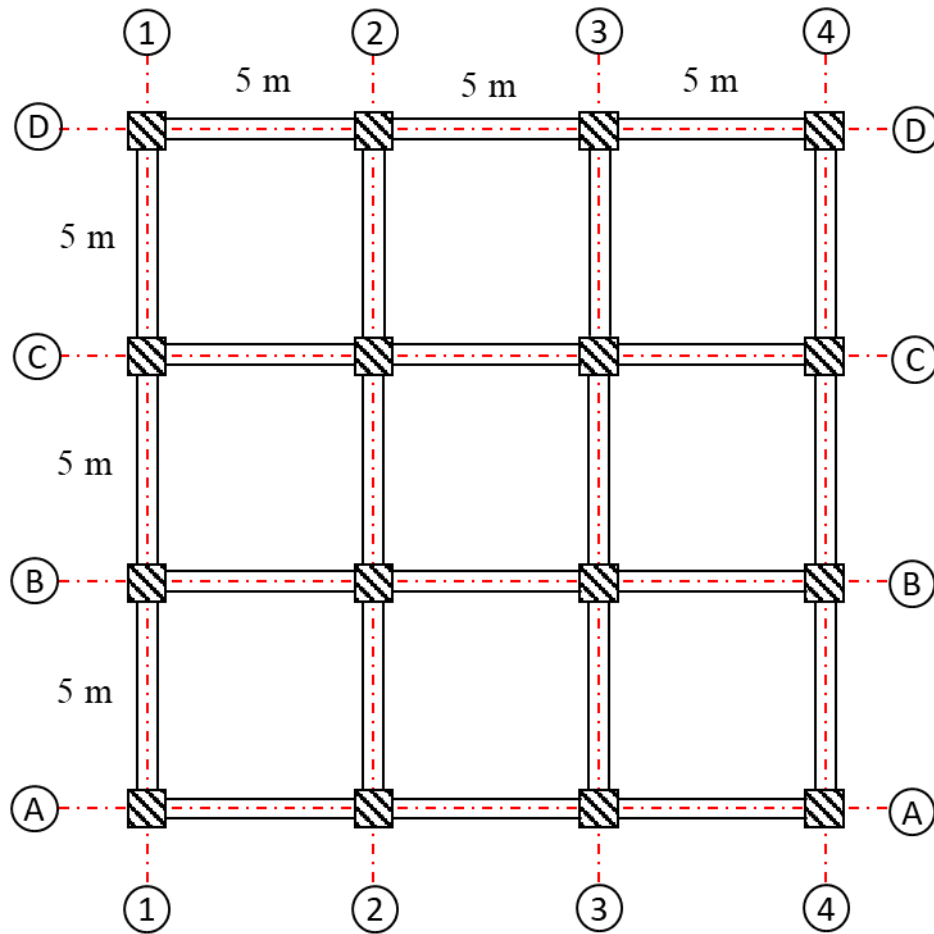


Figure 7: General beam and columns layout

Table 1: Load combinations

Load type	Load Combination
Dead (DL) & Live (LL)	$1.35 DL + 1.5LL$
Dead (DL), Live (LL) & Earthquake ($E_{x,y}$)	$1.0DL + 0.3LL \pm 1.0EX$ $1.0DL + 0.3LL \pm 1.0EY$
Dead (DL) & Earthquake ($E_{x,y}$)	$1.0DL + 0.3LL \pm 1.0EX \pm 0.3EY$

3.3 Materials Definition

The materials assigned for the structural elements in the preliminary conventional RC design, the downgraded vulnerable buildings, and the proposed retrofitting system are

in accordance with the standard quality and assurance control of Eurocode 2 (EN 1992-1-1:2004). Table 2 summarizes the strength and deformation characteristic of the concrete and steel used.

Table 2: Material properties

Structure type	Concrete				Steel				
	f_c MPa	f_{ce} MPa	ϵ_c ‰	ϵ_u ‰	f_y MPa	f_{ye} MPa	f_t MPa	f_{te} MPa	ϵ_u %
Conventional	30	38	2.2	3.5	450	495	607.5	668	9.5
Vulnerable	20	28	2.0	3.5	300	330	375	412	9.0
Retrofitting	35	43	2.25	3.5	450	495	607.5	668	9.5

3.4 Seismic Hazard and Seismicity Parameters

The buildings are designed and evaluated under the influence of seismic activity in accordance with the Eurocode standards. In order to achieve that, type of soil, reference peak ground acceleration (a_{gR}), and the behavior factor (q) are needed to construct the elastic response spectrum representing the seismic actions; which will be used to derive the design forces in the linear design of the conventional vulnerable buildings using the Lateral Force Method of Analysis (LFMA). This elastic spectrum will also be used as a target spectrum for the Nonlinear Dynamic Time-History Analysis (NTHA) to match the seismic hazard of the collected acceleration records to the ones existing at the location under consideration.

3.4.1 Assumed Site Class

The soil is assumed to be of class C consisting of medium dense to dense sand and gravel deposits extending to hundreds of meters below the ground. This type of soil has a shear wave propagation velocity that ranges between 180-360 meters per second, standard penetration resistance between 15 and 50 (i.e., N-value), and average undrained shear strength of 160 kilopascals (EN 1998-1/Table 3.1).

3.4.2 Reference Peak Ground Acceleration

The peak ground acceleration is selected as 0.4g considering a return period of 475 years, which is the highest reference ground acceleration in most of the zonation maps in Europe and its neighboring countries, including Turkey and Cyprus (Solomos et al., 2008). This selection will adequately test the efficiency of the proposed retrofitting system under the impact of severe seismic actions.

3.4.3 Seismic Actions

The seismic hazard at the site of interest considered is assumed to produce ground shaking of high intensity (the site is prone to seismic action with magnitude Mw greater than 5.5), which is represented by Type 1-Elastic Response Spectrum, $S_e(T)$ in EC8 (EN 1998-1/3.2.2.2 (1)P). The elastic spectrum can be defined by the equations below:

$$0 \leq T \leq T_B: S_e(T) = a_g \cdot S \cdot \left[1 + \frac{T}{T_B} \cdot (\eta \cdot 2,5 - 1) \right] \quad (1)$$

$$T_B \leq T \leq T_C: S_e(T) = a_g \cdot S \cdot \eta \cdot 2,5 \quad (2)$$

$$T_C \leq T \leq T_D: S_e(T) = a_g \cdot S \cdot \eta \cdot 2,5 \left[\frac{T_C}{T} \right] \quad (3)$$

$$T_D \leq T \leq 4s: S_e(T) = a_g \cdot S \cdot \eta \cdot 2,5 \left[\frac{T_C T_D}{T^2} \right] \quad (4)$$

where,

T : the natural period of a system

T_B : the lower bound for the constant spectral acceleration segment

T_C : the upper bound for the constant spectral acceleration segment

T_D : the period that defines the starting limit of the constant displacement response range

S : soil factor

a_g : design ground acceleration ($a_g = a_{gR} \times \text{Importance factor}$)

η : correction factor for damping, defined as 1 for 5% viscous damping.

*For soil class C, $T_B = 0.2s$, $T_C = 0.6s$, $T_D = 2.0s$, and $S = 1.15$ (EN 1998-1/Table 3.2).

In order to design the conventional building following the equivalent linear procedure as per EC8, the elastic response spectrum needs to be reduced by a behavioral factor q to account for the overstrength and nonlinear behavior while analyzing the model linearly. The factor q depends on the structural system configuration, the regularity in plan and elevation, importance factor, and ductility class of the structure. All the buildings in this research were designed as regular moment frames classified as Medium Ductile Structures (DCM) with an importance factor of 1. In such structures, q amounts to 3.9 (EN 1998-1/Table 5.1). Given the information above, the reduced design spectrum $S_d(T)$ can be defined using the equations (5-7) (EN 1998-1/3.2.2.5 (4)P). Figure 8 depicts the elastic and the design spectra used in the study.

$$T_B \leq T \leq T_C: S_d(T) = a_g \cdot S \cdot \frac{2,5}{q} \quad (5)$$

$$T_C \leq T \leq T_D: S_d(T) \left\{ \begin{array}{l} = a_g \cdot S \cdot \frac{2,5}{q} \cdot \left[\frac{T_C}{T} \right] \\ \geq 0.2 \cdot a_g \end{array} \right. \quad (6)$$

$$T_D \leq T: S_d(T) \left\{ \begin{array}{l} = a_g \cdot S \cdot \frac{2,5}{q} \cdot \left[\frac{T_C T_D}{T^2} \right] \\ \geq 0.2 \cdot a_g \end{array} \right. \quad (7)$$

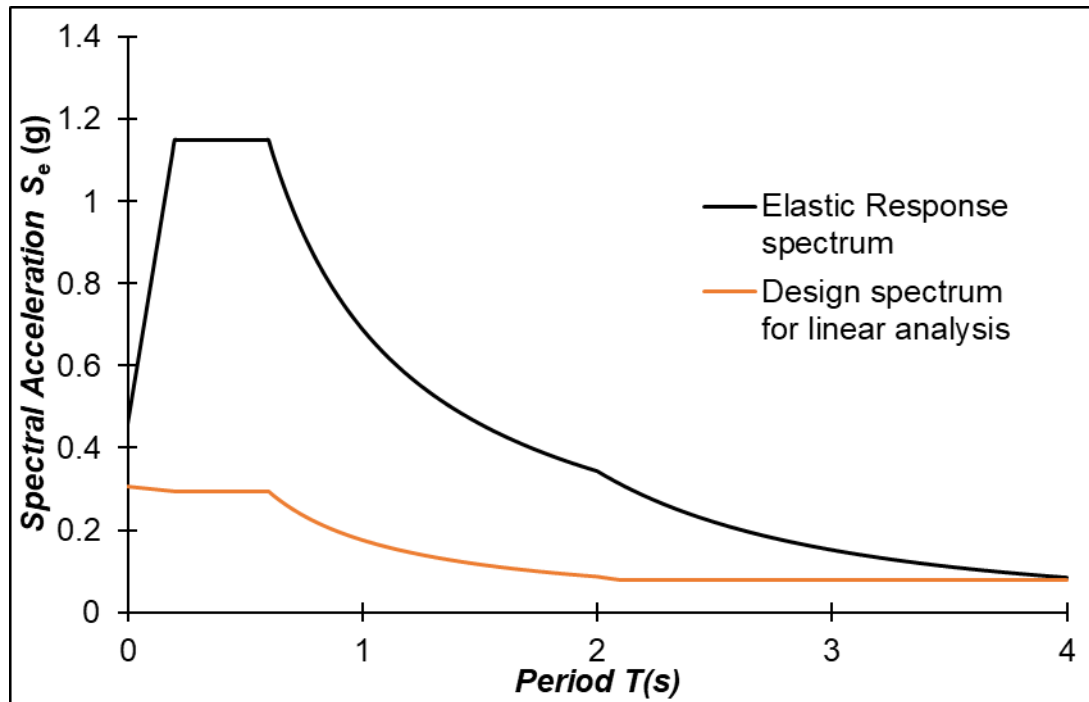


Figure 8: Elastic and design response spectrum

3.5 Ground Motion Records

Selecting suitable ground motion records is a crucial factor in assessing the performance of the existing vulnerable buildings through nonlinear time history analysis. A suite of seven earthquake records, acquired from the Pacific Earthquake Engineering Research Center (PEER) database, was selected to cover a wide range of frequencies and accelerations. Measures were taken to include near-fault, far-fault, as well as records that possess pulse-like frequencies in the selected suite of actual earthquake data. Details of the selected records are given in Table 3, while their actual frequencies and accelerations are presented in Figure 9. Furthermore, these records were scaled to match the elastic target spectrum defined in the previous sections following the approach of minimizing the mean-square error (Michaud & Léger, 2014) and in accordance with EC8 specifications. This method results in a more convenient scaling where it matches the target response without affecting the frequency of the ground motion records. The scaling is carried out for the periods between 0.1 and 2.5s,

covering the fundamental periods for all three types of buildings under evaluation, including the retrofitted ones. The scaled spectrum can be viewed in Figure 10.

Table 3: General information for the chosen ground motion records

Event Name	Year	Fault distance (km)	V_{S30} (m/s)	Magnitude	Duration (sec)	PGA (g)	Record type
Imperial Valley 2	1940	6.09	213	6.95	54	0.27	Near-fault
Imperial Valley 6	1979	7.29	242	6.53	52	0.28	Near-fault
Superstition Hills	1987	18.48	266	6.54	22	0.13	Pulse-like
Spitak Armenia	1988	23.99	344	6.77	20	0.20	Near-fault
Cape Mendocino	1992	41.97	337	7.01	44	0.18	Far-fault
Northridge	1994	6.5	282	6.69	20	0.87	Pulse-like
Taiwan SMART1	1986	55.55	306	7.3	48	0.27	Far-fault

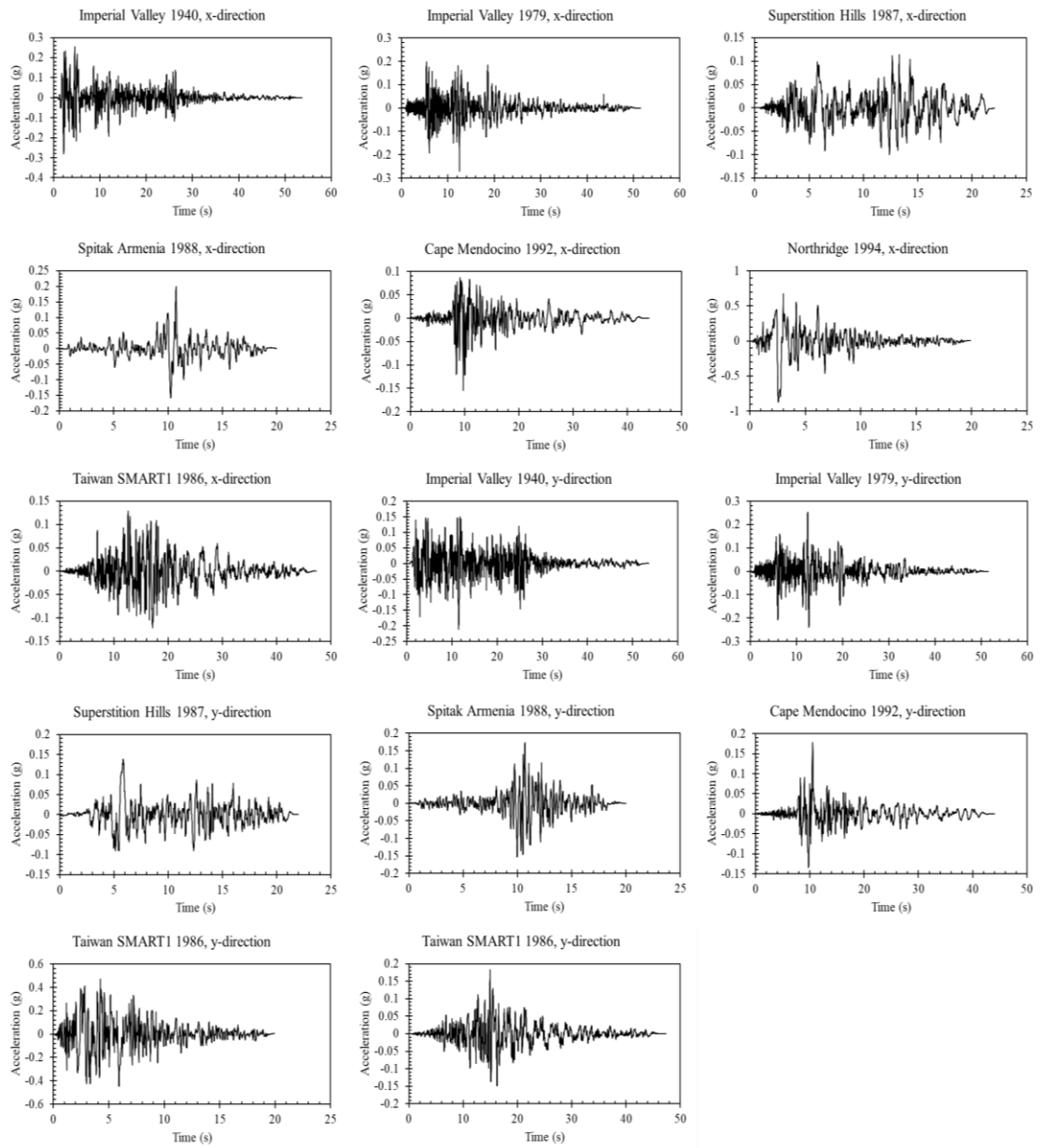


Figure 9: Records frequencies and accelerations

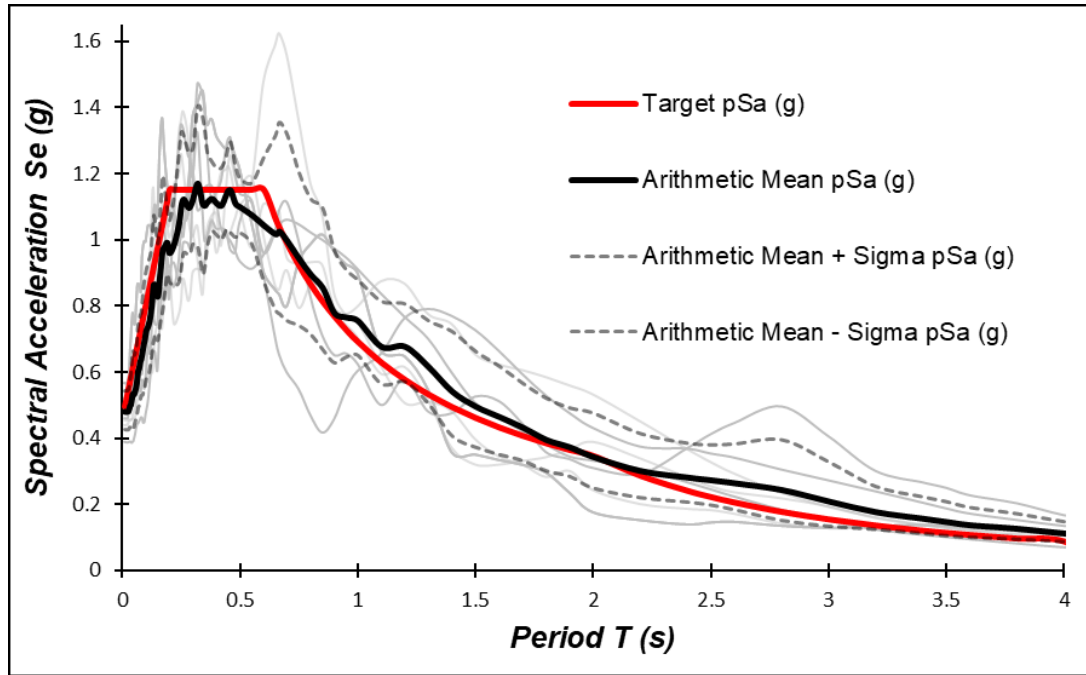
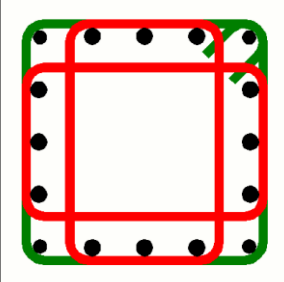
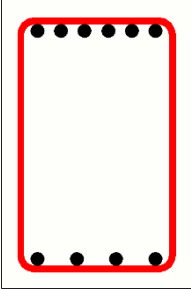
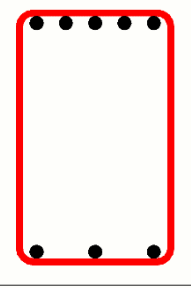
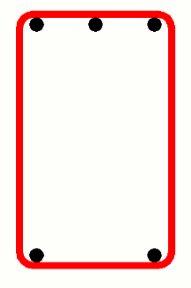
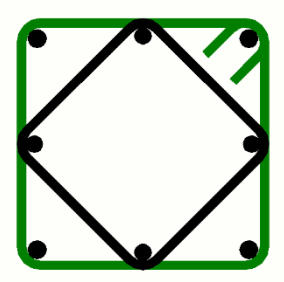


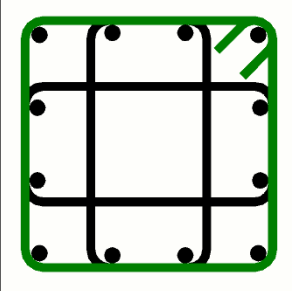
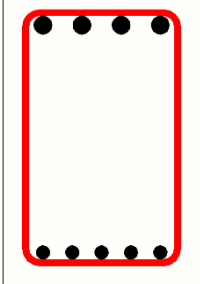
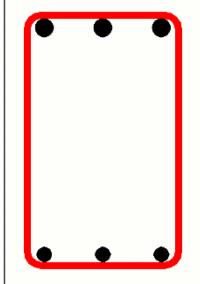
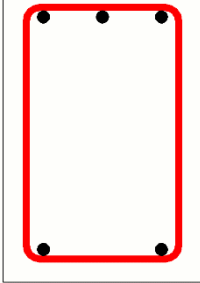
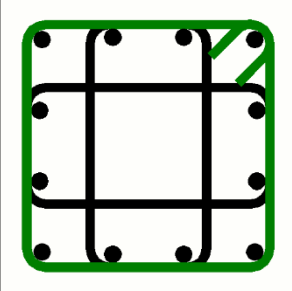
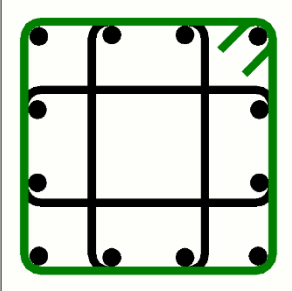
Figure 10: Mean spectral acceleration spectrum for the scaled ground motion records

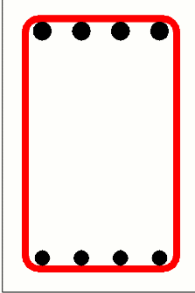
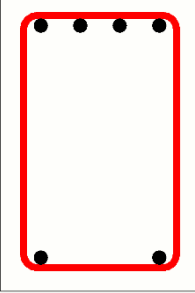
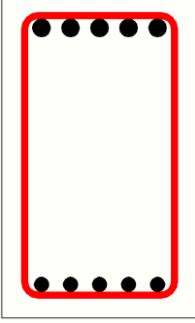
3.6 Vulnerable Building's Cross-Sections

The conventional moment frames were designed in line with Eurocode guidelines and specifications. The sections of the considered vulnerable structures are depicted in Table 4. As shown, all the column has a square cross-section with a concrete cover of 3 cm, while the beam sections mainly have a deep rectangular section to resist the bending stresses acting along their major axis. It is worth noting that the elements cross-section of the 3-story building remained the same for the entire building while the element within the 5 and 7 story buildings are altered at different story levels to produce the most economical design that satisfies Eurocode requirements. Moreover, the reinforcement portrayed in the table shows the detailing along the critical region of the considered element that ensures the development of sufficient local ductility. On the other hand, the slab system was designed as a two-way reinforced concrete slab with a constant thickness of 15 cm in all three buildings.

Table 4: Columns and beams cross-section of the considered vulnerable buildings

Section type	Section layout	Reinforcement details
<p>Column section of 3 story building: 400 × 400</p>		<p>Main reinforcement: 16ϕ16 Transverse reinforcement: 2ϕ8/125</p>
<p>beam section of 3 story building: 300 × 450</p>		<p>Main top reinforcement: 6ϕ18 Main bottom reinforcement: 4ϕ18 Transverse reinforcement: 1ϕ8/145</p>
<p>beam section of 3 story building: 300 × 450</p>		<p>Main top reinforcement: 5ϕ18 Main bottom reinforcement: 3ϕ18 Transverse reinforcement: 1ϕ8/145</p>
<p>beam section of 3 story building: 300 × 450</p>		<p>Main top reinforcement: 3ϕ18 Main bottom reinforcement: 2ϕ18 Transverse reinforcement: 1ϕ8/145</p>
<p>Column section of 5 story building: 400 × 400</p>		<p>Main reinforcement: 8ϕ22 Transverse reinforcement: 2ϕ8/175</p>

<p>Column section of 5 story building: 425 × 425</p>		<p>Main reinforcement: 12ϕ20 Transverse reinforcement: 2ϕ8/150</p>
<p>beam section of 5 story building: 300 × 450</p>		<p>Main top reinforcement: 4ϕ24 Main bottom reinforcement: 5ϕ18 Transverse reinforcement: 1ϕ8/145</p>
<p>beam section of 5 story building: 300 × 450</p>		<p>Main top reinforcement: 3ϕ24 Main bottom reinforcement: 3ϕ20 Transverse reinforcement: 1ϕ8/160</p>
<p>beam section of 5 story building: 300 × 450</p>		<p>Main top reinforcement: 3ϕ16 Main bottom reinforcement: 2ϕ16 Transverse reinforcement: 1ϕ8/130</p>
<p>Column section of 7 story building: 400 × 400</p>		<p>Main reinforcement: 12ϕ20 Transverse reinforcement: 2ϕ10/160</p>
<p>Column section of 7 stories building: 450 × 450</p>		<p>Main reinforcement: 12ϕ24 Transverse reinforcement: 2ϕ10/175</p>

beam section of 7 story building: 300×450		Main top reinforcement: $4\phi 24$ Main bottom reinforcement: $4\phi 20$ Transverse reinforcement: $1\phi 8/160$
beam section of 7 story building: 300×450		Main top reinforcement: $4\phi 18$ Main bottom reinforcement: $2\phi 18$ Transverse reinforcement: $1\phi 8/145$
beam section of 7 story building: 300×500		Main top reinforcement: $5\phi 24$ Main bottom reinforcement: $5\phi 20$ Transverse reinforcement: $1\phi 8/160$
*The dimensions are shown in mm in this table		

3.7 Proposed Retrofitting System

This research proposes a peripheral frame to retrofit an existing vulnerable building as a non-destructive approach. The system basically confines the existing structure with an external rigid frame. The point of contact between the existing structure and the peripheral frame is modeled using a gap link with a zero spacing and a stiffness approaching infinity. It should be noted that the peripheral frame columns are connected with each other by means of reinforced concrete tie beams at the same level of the existing building slabs. Schematic view of the proposed system is presented in Figure 11.

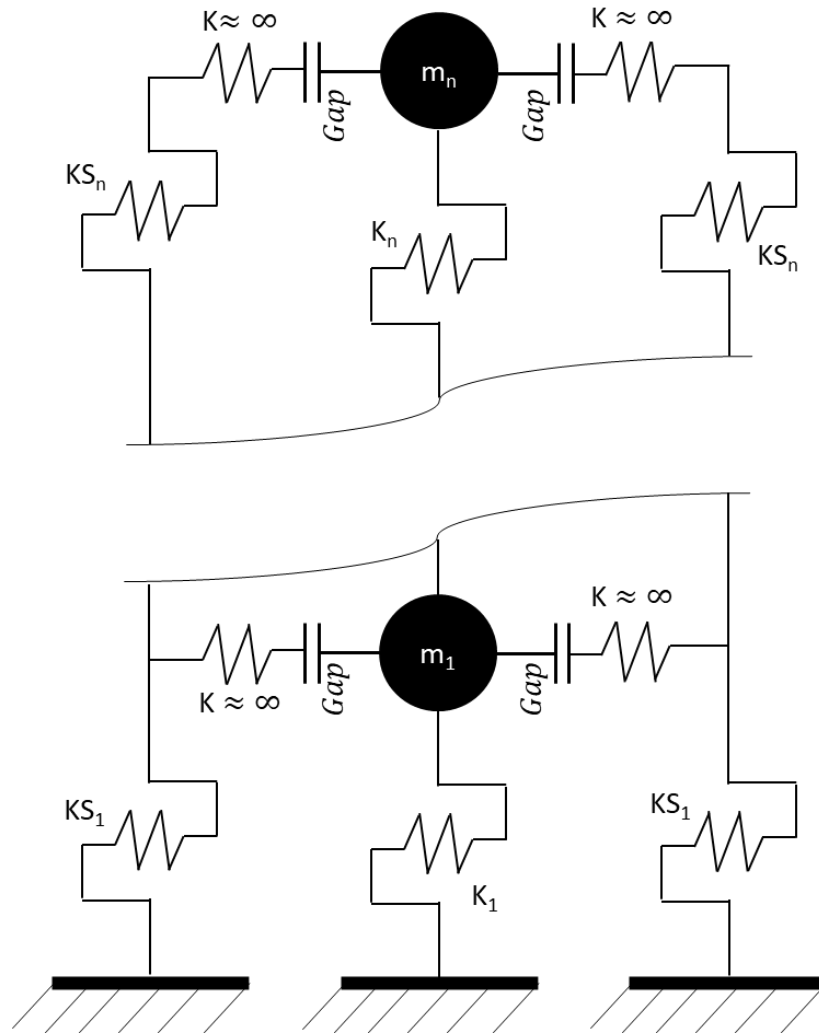


Figure 11: Idealized schematic view of the proposed retrofitting system

3.8 3D Modeling of The Buildings

CSI-ETABS V19.0 was used to construct and analyze a three-dimensional (spatial) Finite Element model with the plan and details mentioned above. All the structural models handled by the program fulfill the requirements of EN 1998-1/4.3.1-2. The fundamental characteristics of the elastic models can be summarized as follows:

- All frame elements are modeled as rigid line elements. The external walls are considered in the analysis as additional dead load acting on the beam.
- The slabs have been modeled and analyzed as thin-shell elements with appropriate meshing sizes to ensure accuracy.

- Rigid diaphragms were defined along the horizontal frames connecting all the nodes located at the same level (height).
- Rigid offset was considered in the panel zone at the beam-column connection. The columns were assumed to be fully rigid, i.e., having a factor of 1, and the beams had a zero factor, meaning that the lateral stiffness will come essentially from the columns.
- All structural elements are fully fixed at the base.
- Cracked sections are considered in all concrete elements following EN 1998-1/4.3.1(6). Consequently, the Poisson's ratio has been taken as 0 for concrete material.
- As per EN 1998-1/4.3.1(7), the flexural stiffness for beams, columns, and slabs was modified to be equal to 50% of the corresponding stiffness of uncracked sections.
- The effect of accidental torsion was taken into consideration in the design by accounting for 5% eccentricity when calculating seismic forces in both x and y directions as stated in EN 1998/4.3.3.3.
- The rigid moment frames are the sole source of lateral resistance in the model as the effect of infill walls is ignored.
- All the models have been initially designed to pass the regularity criteria in plan and elevation described in EN 1998-1/4.2.3.2, and EN 1998-1/4.2.3.3 respectively.
- The mass source considered in the analysis is taken as the self-weight of the structural system plus the additional dead load and 30% of the imposed live load.

3.9 Nonlinear Modeling

This section presents the basic concepts of inelastic computer modelling used to construct the nonlinear models of the structures under evaluation. Most of the fundamental steps for the inelastic modelling are similar to those mentioned in section 3.8 however the following underlying assumptions are considered to convert the elastic models to ones capable of representing the actual nonlinear behavior of the structure in order to guarantee a detailed performance evaluation.

In general, the overall structural stiffness is a function of material properties, cross-sectional dimensions, and member geometry and configuration. These properties are interconnected in a hierarchical form, with the material being at the apex of the chain. Accordingly, the effects of nonlinearity beyond yielding can be introduced to the mathematical model either at material, cross-sectional, or member levels to formulate the structural stiffness used to capture the local and global inelastic phenomenon. For this purpose, the complete stress-strain curves for the materials used were defined, as shown in Figure 12, instead of only using the constant elastic properties in order to simulate all modes of deformation experienced by the structure and account for the nonlinearity from the onset of loading to the end of seismic action. Mander's model was used to define the curves for the concrete both for confined and unconfined regions (Mander et al., 1988), while park model was used for the reinforcement (Park & Paulay, 1991). Furthermore, Rayleigh damping is utilized for the nonlinear direct integration analysis in ETABS. Rayleigh coefficients (alpha and beta) are selected such that 5% damping ratio is employed at vibration periods equal to 1.5 and 0.25 times the fundamental period of the structure to properly depict the inherent damping commonly present in an RC structure.

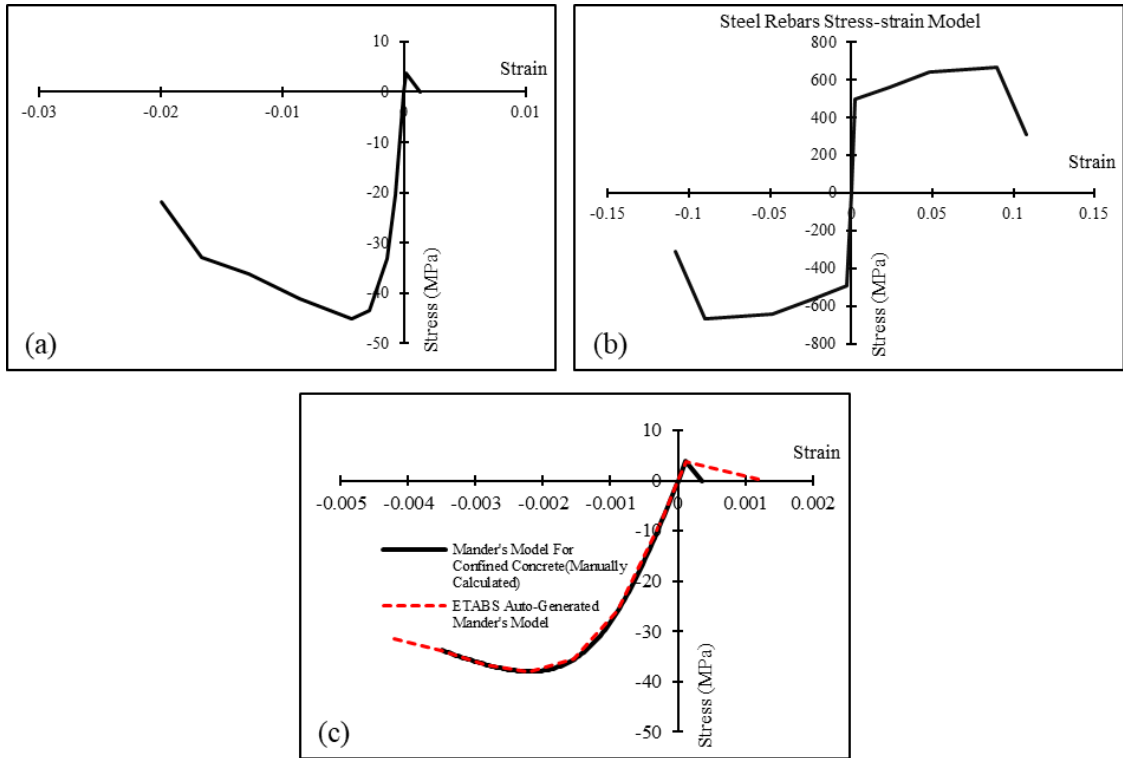


Figure 12: A sample of the Stress-strain relationship curves used in the analysis of the of the 3-story building. (a) Stress-strain curve of the confined concrete used for the columns, (b) the Stress-strain curve for the reinforcement, (c) the Stress-strain curve

3.9.1 Concentrated Inelasticity Fiber Modeling

In this study, the adopted idealized nonlinear modeling technique is known as The Concentrated Inelasticity technique, as per ATC 70 (2010). This technique utilizes uniaxial fiber hinges that can explicitly capture some features of the nonlinear behavior according to the nonlinear stress-strain curves of materials, while other effects are considered by integrating the flexural stresses developed over the cross-section of the element and along the fiber's length. In this modeling approach, a single cross-section consisting of discretized fibers is used along a fraction of the member's length, mainly where the inelastic action is anticipated (Figure 13), which is typically located at the ends of the elements in RC moment frames. For reinforced concrete beams and columns, a fiber segment may be composed of several discrete concrete and steel

reinforcements fibers given their respective stress-strain relationships. The number of fibers used in each cross-section heavily influences the accuracy of the analysis; however, based on previous data available on NIST guidelines (2017), an optimal number of 56 for the beams and 28 fibers for the columns is used to ensure accurate results with a minimal computational burden as depicted in Figure 14. Moreover, the critical plastic hinge length (L_p) for each element over which the nonlinear deformations are concentrated is calculated following the proposed expression by Berry and Eberhard (2008).

$$L_p = 0.05L + 0.1 \frac{f_y d_b}{\sqrt{f'_c}} \leq \frac{L}{4} \quad \text{Eq(8)}$$

where,

L : total length of the structural element

f_y : yield strength of reinforcement in MPa

d_b : main reinforcement diameter in the section

f'_c : characteristic compressive strength of concrete.

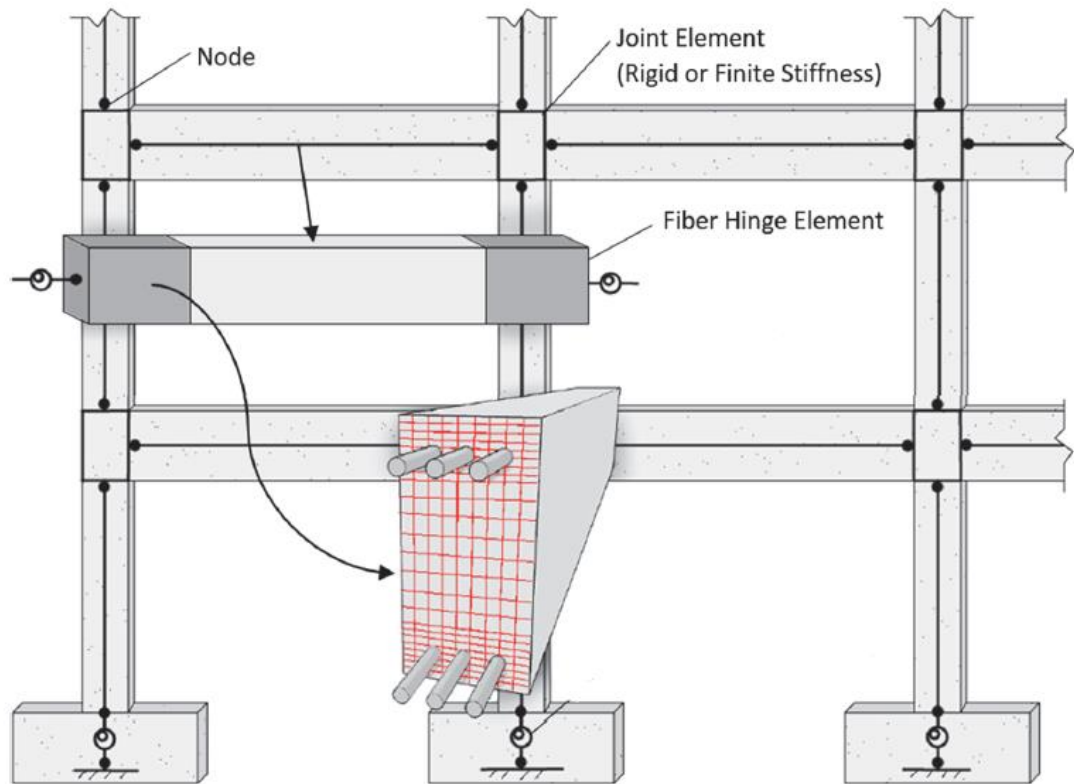


Figure 13: Illustration of a typical fiber-type modeling for reinforced-concrete moment- frames. (NIST, 2017)

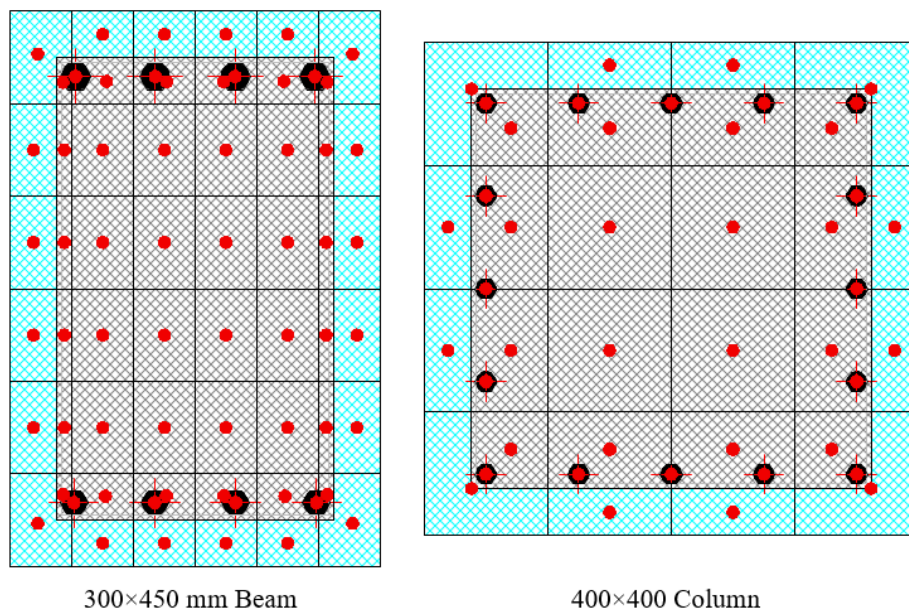


Figure 14: Discretization of Fibers in Beams and Columns

Finally, based on the work of Kwon (2016), the stiffness modification factor (which was 0.5 in the elastic models) was adjusted for beams and columns to account for the potential bar slip phenomenon, cracked concrete section, reinforcement ratios, and axial load ratios. The reduction factor (α) can be calculated as:

$$\alpha = 0.003 \times IDR^{-0.65} + \gamma \leq 0.8 \quad \text{Eq(9)}$$

$$\gamma = (-50\rho_T + 2.5) \left(\frac{P}{A_g f'_c} \right)^{(-200\rho_T + 219)} + (15\rho_T + 0.05) \quad \text{Eq(10)}$$

where,

IDR: inter-story drift ratio. For moment resisting frames 0.8% IDR can be used to estimate member stiffness at first yield.

A_g : member's total cross-sectional area

f'_c : characteristic compressive strength of concrete.

ρ_T : longitudinal tension reinforcement ratio

3.9.2 Calibration of The Gap Elements

The connection interface between the existing structure and the retrofitting peripheral encasement has been modeled using nonlinear link elements of type Gap. Gap elements simulate the contact between the outer elements of the venerable building and the strengthening frames by creating restoring forces when the elements are in contact and removing them when the elements move away from each other. Therefore, the gap should inherently have a large stiffness when the surfaces are in touch and zero when they are separate as depicted in Figure 15. The nonlinear gap stiffness is a key parameter in the analysis as it often controls the solution of the entire equation of motion. It is often tempting to define a very large stiffness value as recommended in many published research; however, too large stiffness may lead to numerical difficulties in the analysis due to a phenomenon called Bouncing in which the state of

the gap interchanges back and forth (closed/open) with each iteration of the solution (Rizzo, 1991).

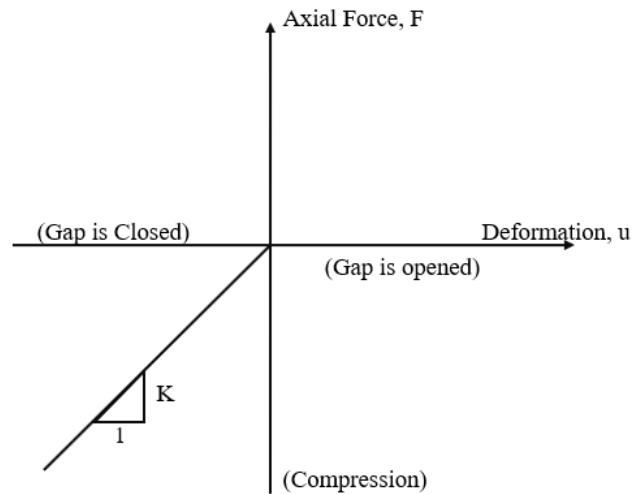


Figure 15: The force-deformation relationship in gap elements

Calibration has been done to select the most appropriate stiffness value for the gap elements to deliver accurate results without sacrificing much time. This was achieved by creating a retrofitted building model and subjecting it to arbitrary lateral loading. By gradually increasing the stiffness of the gap elements and monitoring the forces generated and displacement encountered at one of the nodes, it was clear that choosing a stiffness 100 times (two orders of magnitude) greater than the corresponding stiffness of any connected elements is sufficient to obtain reasonably accurate results as quickly as possible. It should be noted that this value was also one of the recommended stiffness values highlighted by CSI ETABS analysis reference (2019).

Chapter 4

RESULTS AND DISCUSSIONS

4.1 Introduction

Within this chapter, the results obtained from the finite element simulation by means of linear and nonlinear structural analysis are presented together with a comprehensive explanation regarding the observed seismic behavior and performance of the proposed retrofitting technique. The key characteristics of seismic demands and performances discussed are; roof displacement, roof acceleration, drift ratios, total energy components, and nonlinear hinge state.

4.2 Seismic Vulnerability Investigation

As mentioned in Chapter 3, the first stage in the study was to conduct a preliminary economic design for the selected buildings in line with the Eurocodes standards. Table 4 shows the adequate cross-sections and reinforcements details that satisfied all the capacity and strength requirements. After that, the structures were weakened by reducing the materials' strength (Table 1, Chapter 3), and linear analysis employing the Equivalent Lateral Force Method was used to investigate the vulnerability of the structure under seismic actions.

For the 3-story building, the preliminary design was deemed seismically weak without even weakening the materials despite passing the capacity checks for the linear analysis, as can be seen in Figure 16. This judgment was encouraged because all of the base columns barely passed the capacity checks as the demand/capacity (D/C) ratios

for PMM interaction were approximately equal to one. Later on, this decision was supported by the findings of the nonlinear analysis which showed that the hinges formed did not meet the limit states to ensure life safety in the event of strong earthquakes.

Whereas upon weakening the 5-story and 7-story buildings, the linear analysis helped identify many members prone to failing under the application of lateral loading, the deficiencies identified are portrayed in Figures 17 and 18. BCC stands for Beam to column capacity ratio deficiency, implying that the columns are likely to reach their limit and fail before the beams do, which is extremely unfavorable for buildings and can lead to catastrophic outcomes. On the other hand, PMM indicates that the member is overstressed and fails to handle the combination of moments and axial loads developed due to the gravity and seismic loads. Thus, all three buildings were considered seismically weak, and the need for seismic retrofitting has been justified and confirmed.

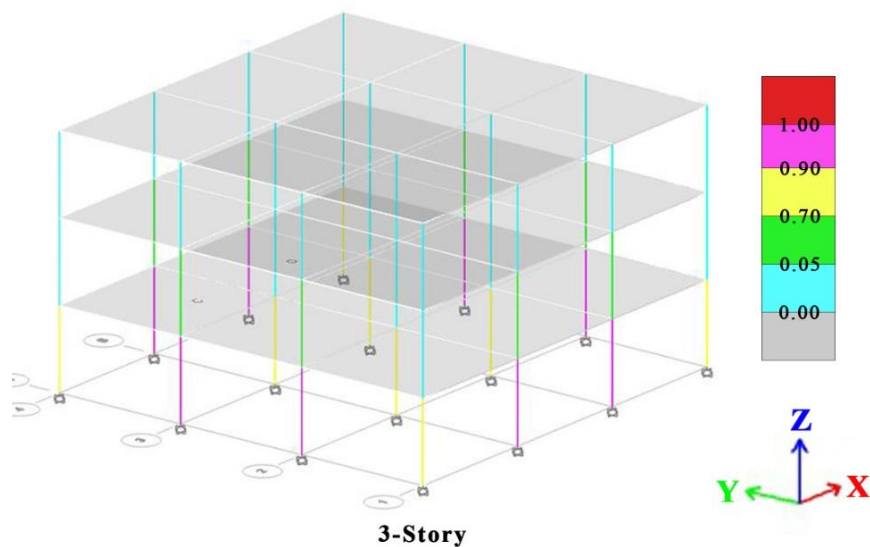


Figure 16: Linear analysis Demand/Capacity checks for column PMM ratio in the 3-story bare structure

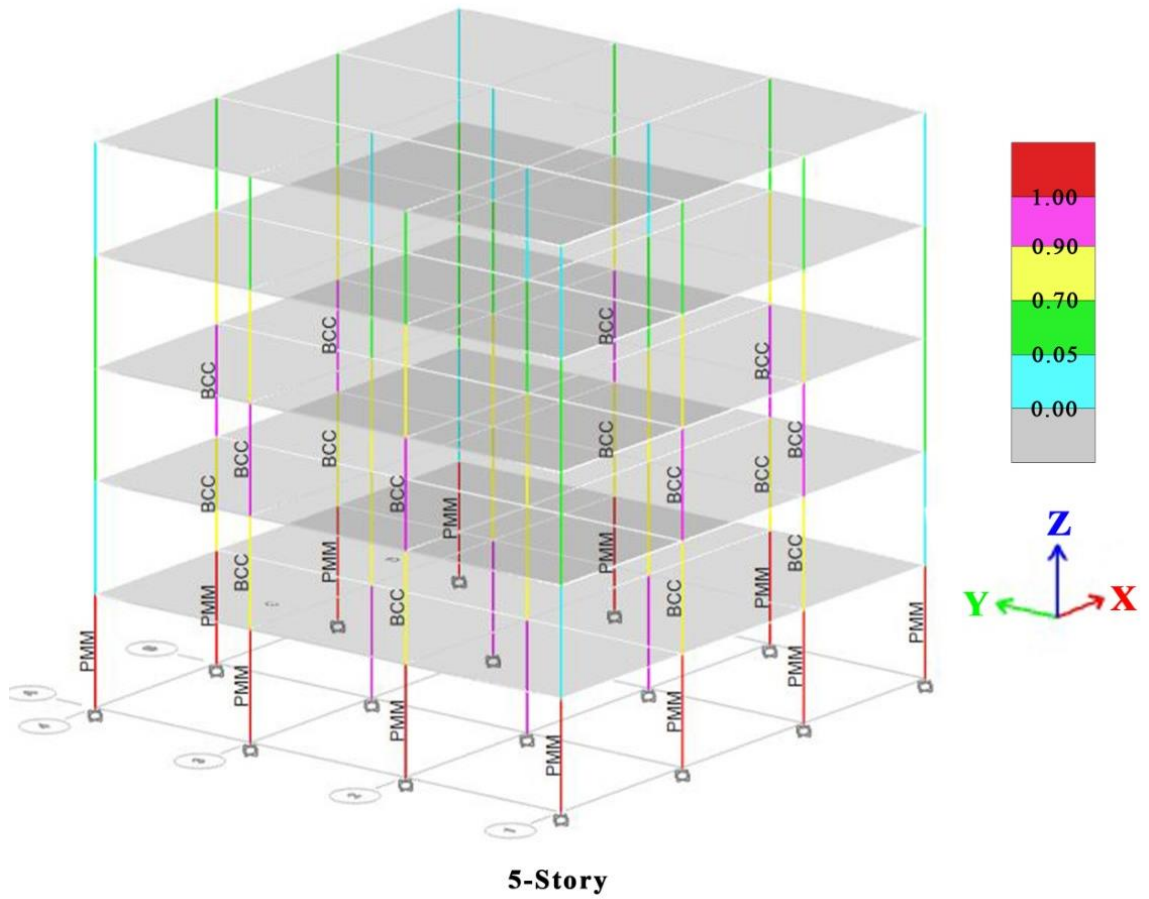


Figure 17: Deficiencies identified by the linear analysis of the 5-story bare structure

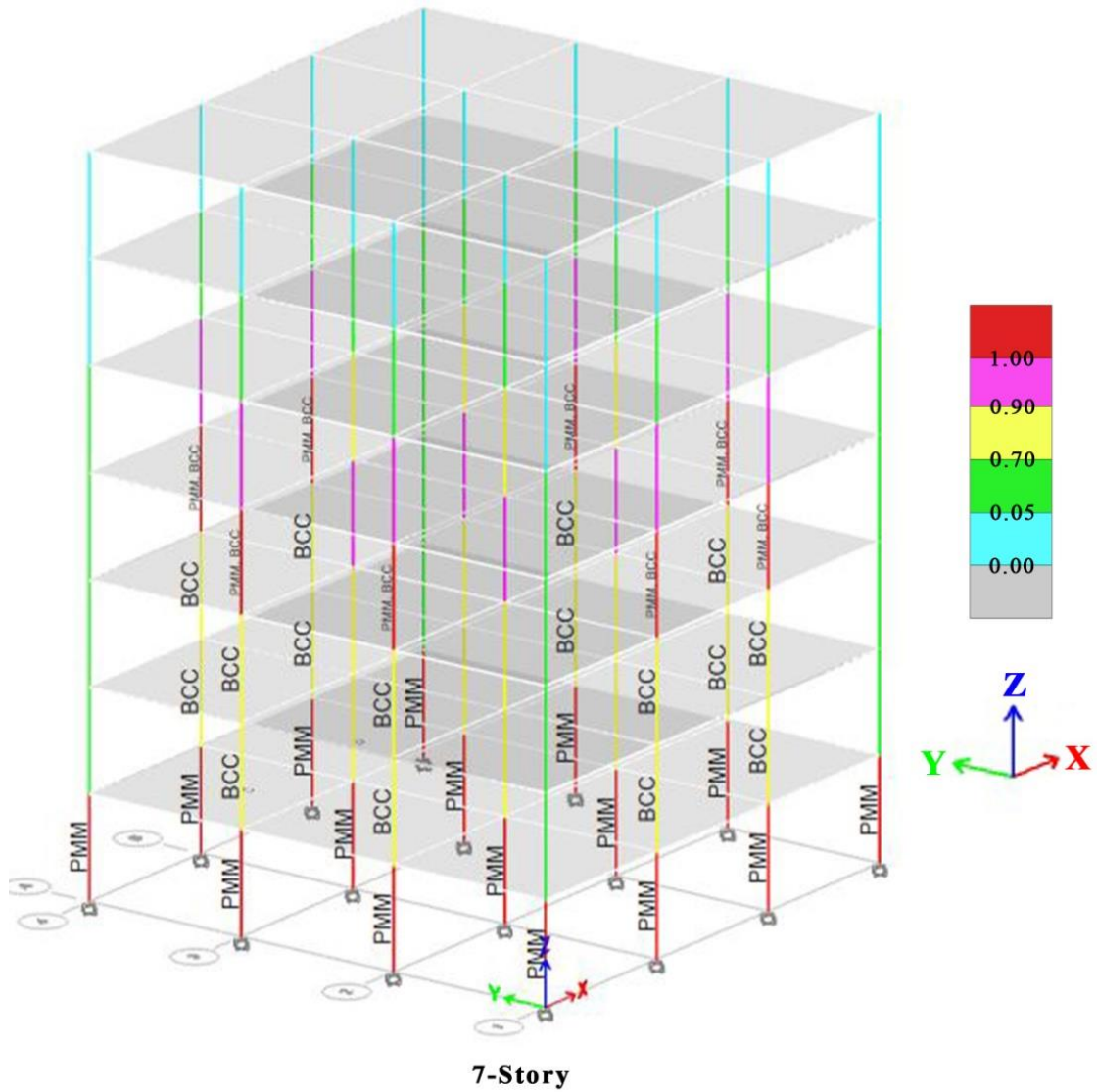


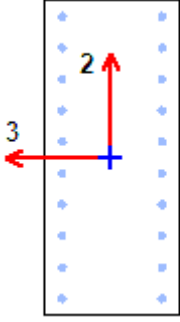
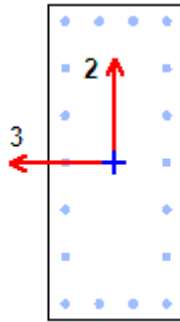
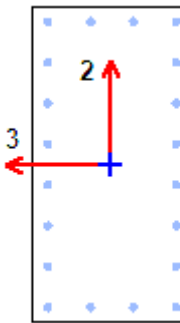
Figure 18: Deficiencies identified by the linear analysis of the 7-story bare structure

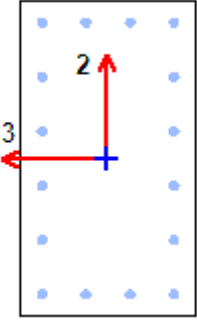
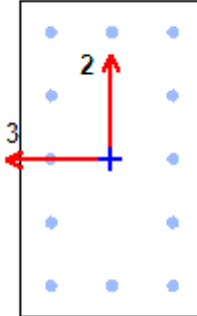
4.3 The Proposed Retrofitting System

Once the bare structures have been categorized as seismically weak, the proposed retrofitting plan commenced. A set of nonlinear models for the bare structures, referred to as vulnerable structures hereafter, has been constructed as Finite Element Models in ETABS and analyzed using direct integration Nonlinear Time History Analysis (NTHA) applying the earthquake records given in section 3.6 in order to produce a basis upon which the efficiency of the retrofitted system will be assessed. After that, the integrated retrofitting system comprising the addition of encasement frames to

enhance the seismic capacity of the vulnerable structures has been modeled nonlinearly (Figure 19). As mentioned previously, cycles of NTHA were performed to obtain the optimum cross-sections and the corresponding reinforcement details for the encasement members. The cycles started with a uniform dimension of 800×250 mm for the beams and columns, and Table 5 shows the final acquired geometry and detailing requirements for the retrofitting elements that satisfy Eurocode8 provisions and meet the performance objectives to minimize damage to structural members.

Table 5: Optimized column cross-sections for the proposed retrofitting system

Section type	Section layout	Reinforcement details
Column section of 3 story building: 950×400		Main reinforcement: $20\phi 22$ Transverse reinforcement: $2\phi 10/100$
Column section of 5 story building: 1000×425		Main top reinforcement: $18\phi 26$ Transverse reinforcement: $2\phi 10/100$
Column section of 7 story building (1 st , 2 nd , & 3 rd story): 1100×550		Main top reinforcement: $20\phi 26$ Transverse reinforcement: $2\phi 10/100$

<p>Column section of 7 story building (4th & 5th story): 900 × 500</p>		<p>Main top reinforcement: 16ϕ26 Transverse reinforcement: 2ϕ10/100</p>
<p>Column section of 7 story building (6th & 7th story): 600 × 350</p>		<p>Main top reinforcement: 12ϕ20 Transverse reinforcement: 2ϕ10/100</p>
<p>*The dimensions are shown in mm in this table * 2 and 3 red arrows indicate the major and minor axes of the section</p>		

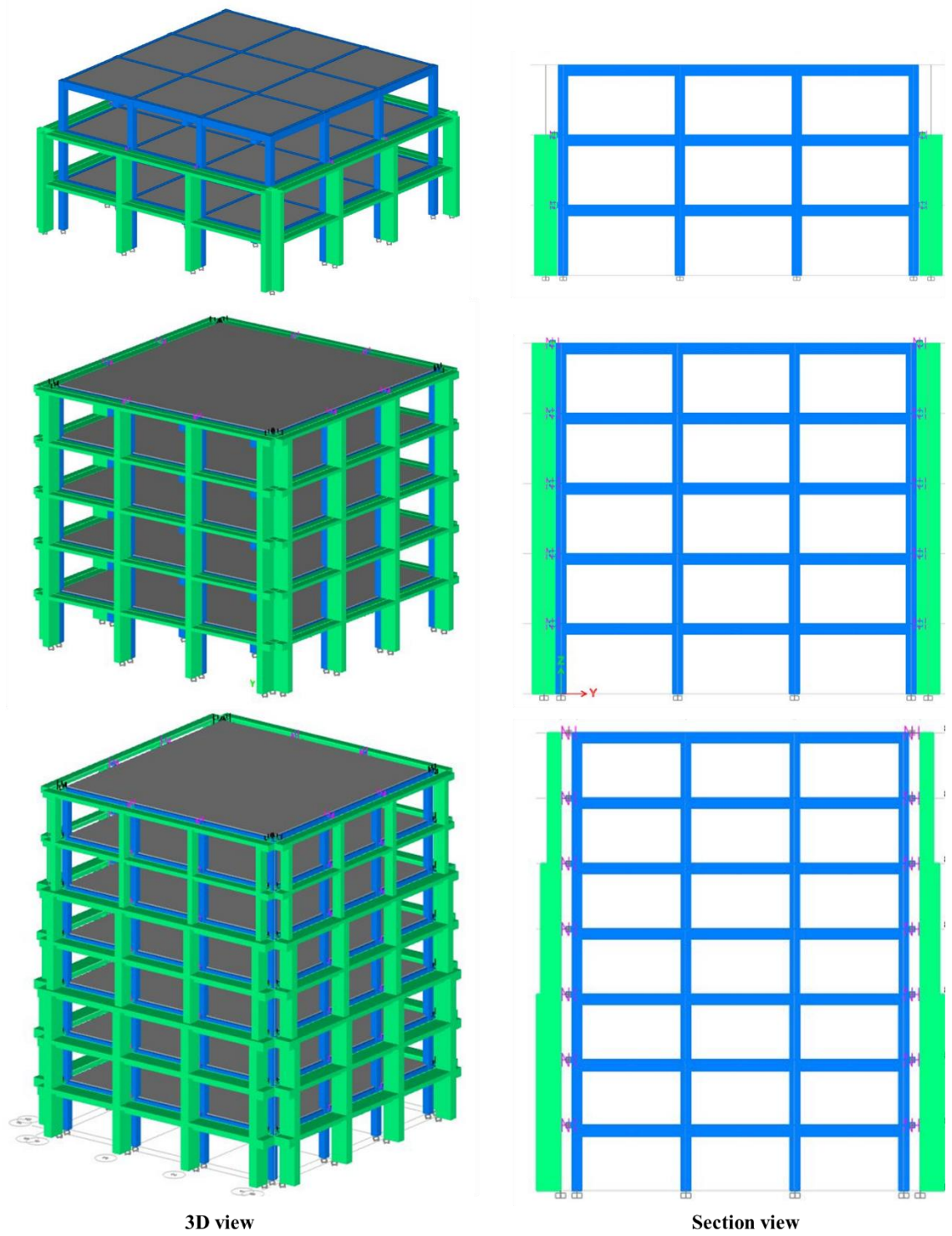


Figure 19: 3D models of the proposed retrofitted structures and their section view

4.4 Seismic Behavior of structures

This section will report the results obtained from analyzing the nonlinear models. As part of this study, the performance will be investigated in terms of global and local responses. Global responses include the fundamental vibration periods of the structures, maximum lateral roof displacement, roof acceleration, and drift ratio. Whereas local or element level responses are determined by inspecting the nonlinear behavior and the limit states of the hinges throughout the period of loading.

4.4.1 Global Responses

4.4.1.1 Fundamental Periods

The modal analysis resulted in the fundamental periods presented in Table 6. It is of interest to note that Eigenvalue modal analysis has been carried out for the linear models while Ritz vector analysis has been implemented to estimate the modal response for the retrofitted models, which essentially behaves nonlinearly. The ritz vector approach was performed considering a starting load vector containing a set of loads that triggers the nonlinear inner deformation of the nonlinear link elements used to connect the retrofitting system to the existing vulnerable structure. The purpose of such vectors is to develop Modes capable of representing the nonlinear behavior of the structure.

Table 6: Fundamental periods of structures

Number of Stories	Structure type	Period (s)
3	Vulnerable	0.706
	Retrofitted	0.512
5	Vulnerable	1.238
	Retrofitted	0.727
7	Vulnerable	1.602
	Retrofitted	0.883

As expected, the buildings' periods were shortened after incorporating the proposed retrofitting system. This means that the mass/lateral stiffness ratio was reduced even though more conservative values for stiffness modifiers were used (i.e., more reduction in stiffness following Eq (9)) in the nonlinear analysis to account for the cracking, axial load ratios, and reinforcement ratios. In other words, the lateral stiffness of the retrofitted structure has been significantly increased in all three buildings under evaluation.

4.4.1.2 Roof Displacement

Perhaps the most transparent way to assess the global behavior of the structure is to examine the maximum deformation occurring under the excitation from the different earthquake events considered in the nonlinear analysis. Tables 7, 8, and 9 report the maximum (and the minimum in the negative direction) displacement experienced at the structure's roof for the 3-story, 5-story, and 7-story buildings, respectively; each table contains a comparison between the vulnerable and the retrofitted buildings in both horizontal directions.

For the 3-story building, the vulnerable structure has undergone a maximum lateral displacement of 168.281 mm in the x-direction and 153.553 in y-direction under the input of "Imperial valley 06" earthquake and "Northridge-01" earthquake, respectively. The corresponding response of the retrofitted structure was significantly lower under the same earthquake records as the maximum roof deformation in the x-direction in the case of "Imperial valley 06" was reduced by 92.801 mm, whereas in y-direction, the response to "Northridge-01" earthquake was 40.707mm lower. This was the common trend seen in all of the data obtained from the earthquake events considered except for "Cape Mendocino" where the retrofitted structure suffered

slightly increased roof displacements but without exceeding the elastic limits and leaving permanent damage.

In the case of the 5-story building, the vulnerable structure was subjected to a maximum lateral deformation of 309.066mm in x-direction and -379.391 in y-direction. The responses to the same ground motion were reduced in the strengthened building by 143.877 mm and 263.828mm, respectively. This huge margin of reduction is due to the retrofitting peripheral encasement covering the structure at all levels as opposed to partial confinement provided in the 3-story building (Figure 20, and 21).

Moreover, in the 7-story building, a huge reduction in the maximum roof displacement was also observed under the same load conditions as the lateral deformation dropped from 398.247mm to 346.078 mm in the x-direction, and from -493.042mm to -220.215 in the y-direction. An example of the roof deformation time history in response to "Imperial Valley-06" earthquake record can be seen in Figure 22.

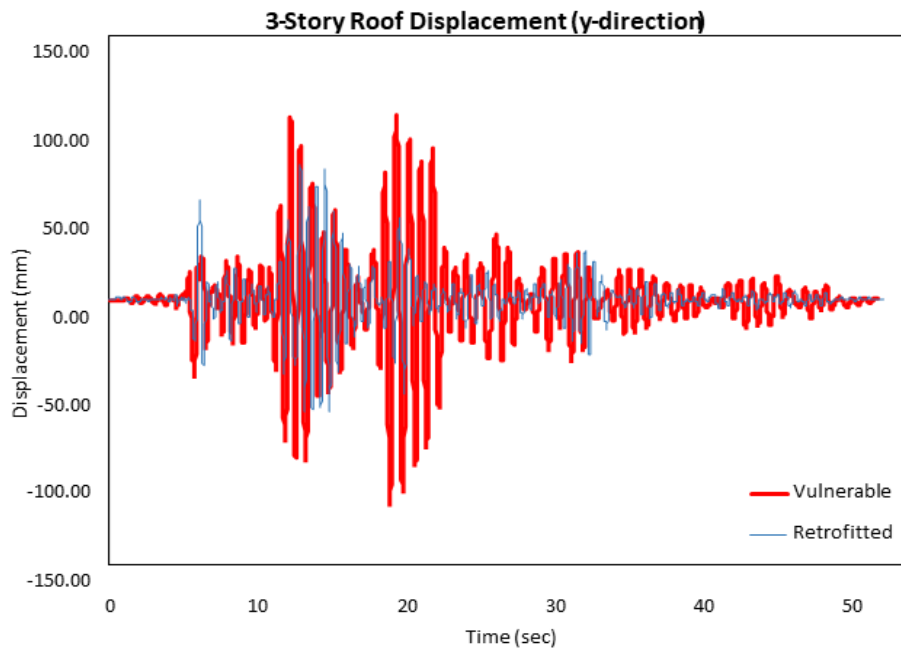
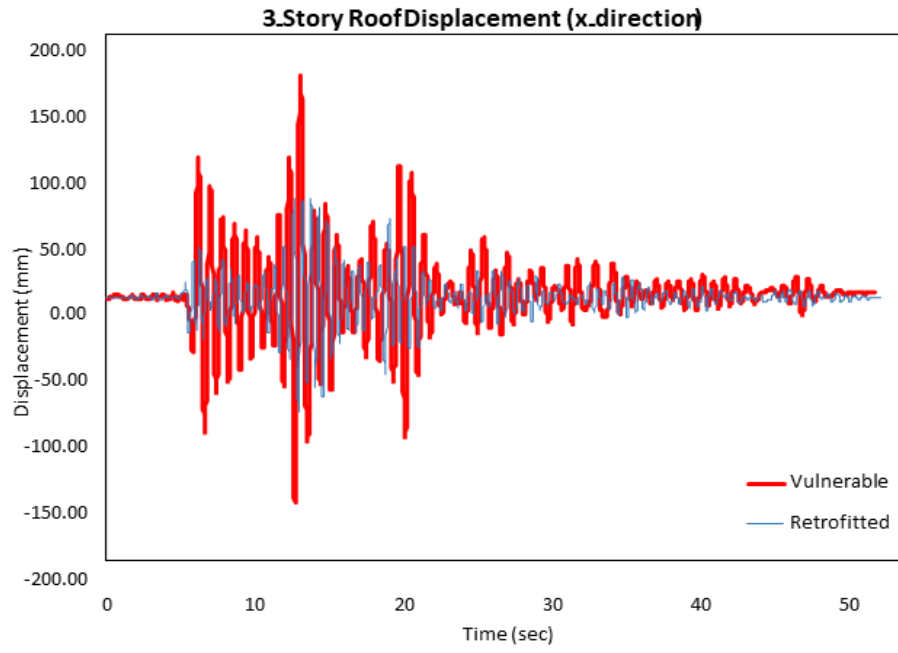


Figure 20: 3-story buildings' roof displacement time history in response to "Imperial Valley-06" earthquake record

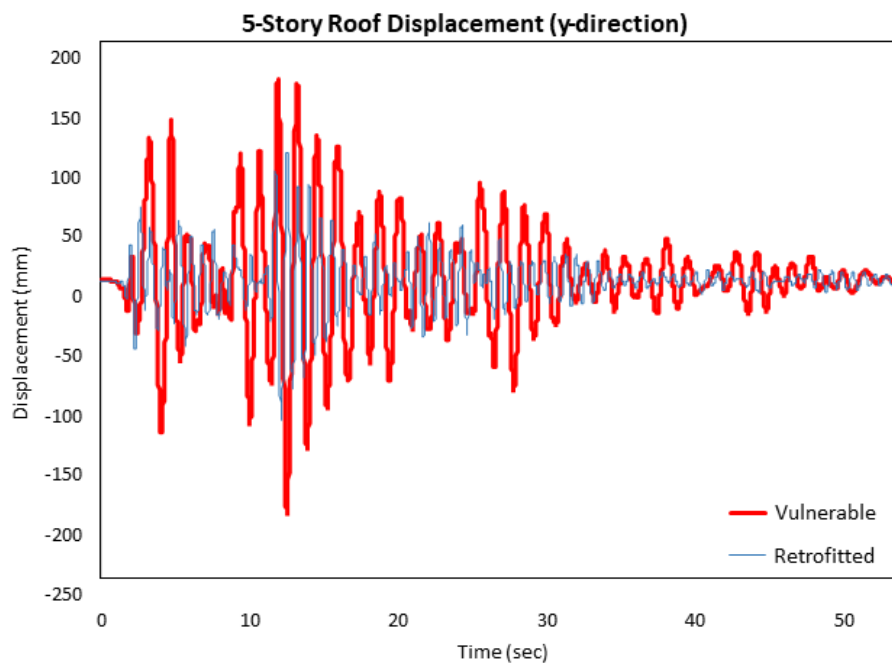
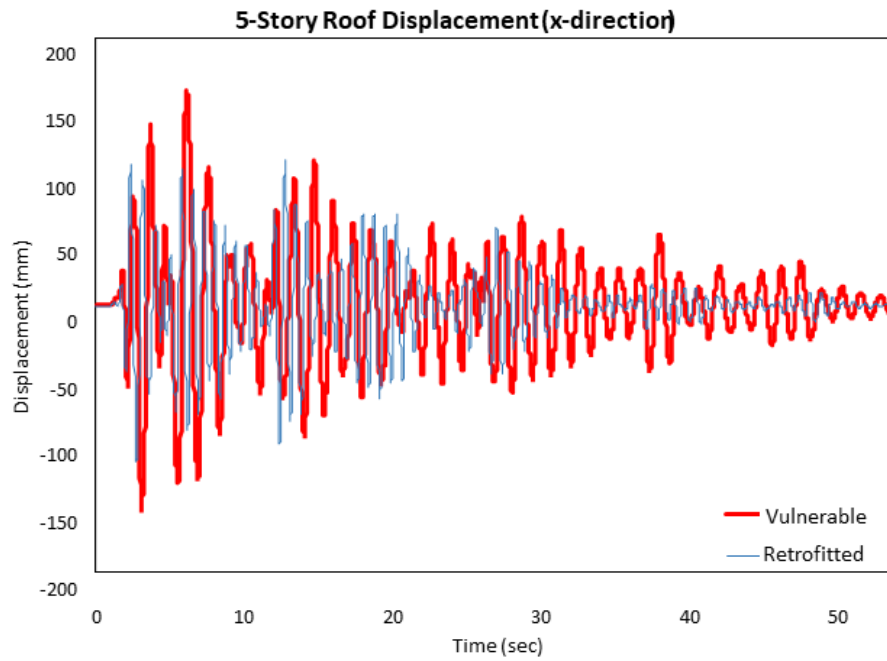


Figure 21: 5-story buildings' roof displacement time history in response to "Imperial Valley-02" earthquake record

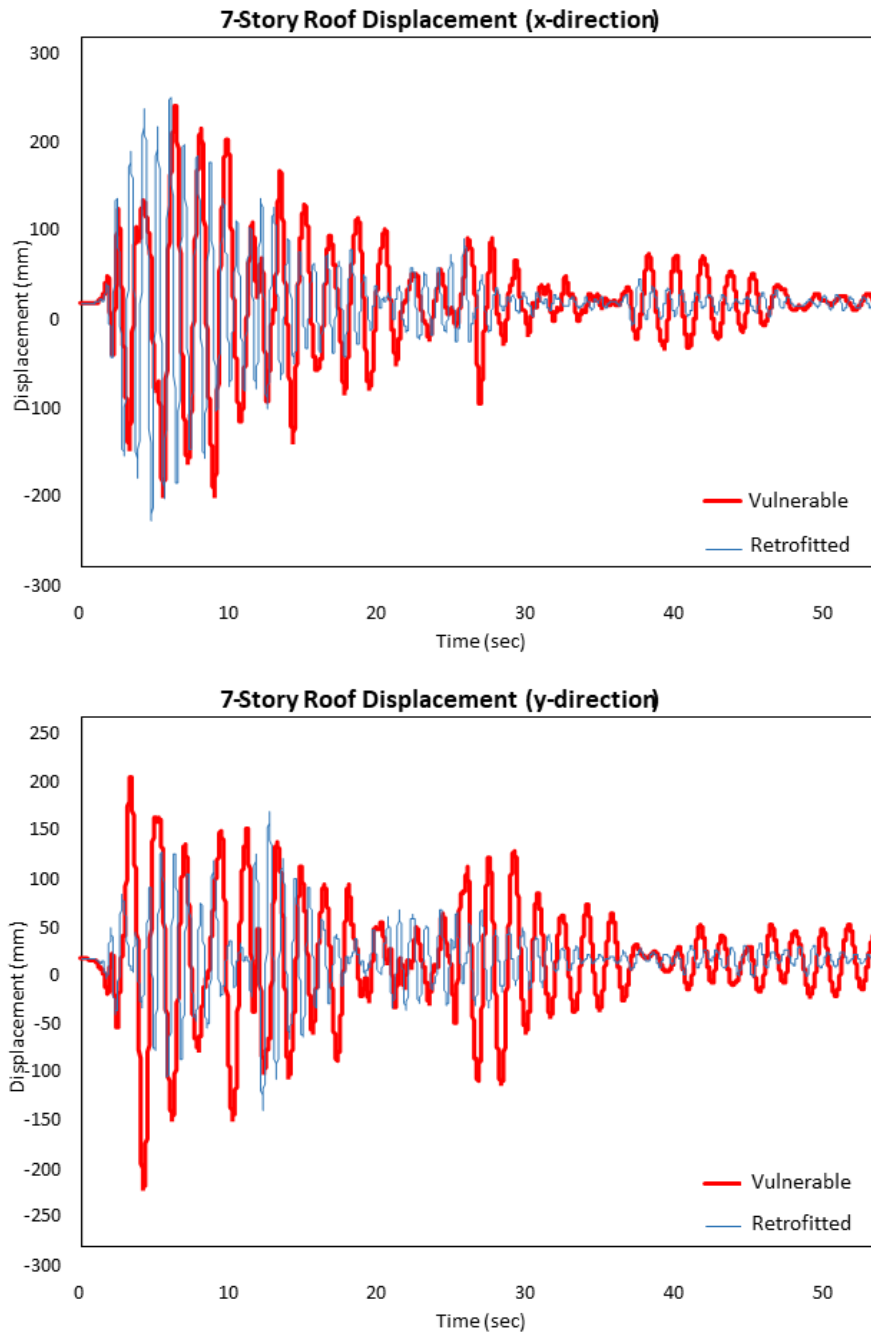


Figure 22:7-story buildings' roof displacement time history in response to "Imperial Valley-02" earthquake record

Table 7: Maximum roof displacements for 3-story structures

Earthquake Event		Vulnerable		Retrofitted	
		X Direction (mm)	Y Direction (mm)	X Direction (mm)	Y Direction (mm)
Northridge-01	Max	52.247	153.553	77.644	40.707
	Min	-70.026	-148.292	-69.649	-43.019

Cape Mendocino	Max	63.307	82.548	64.345	77.12
	Min	-59.949	-70.937	-65.834	-102.881
Spitak Armenia	Max	64.332	114.709	75.018	81.708
	Min	-45.259	-145.77	-64.699	-85.008
Superstition hills 02	Max	97.422	117.493	68.841	77.294
	Min	-87.27	-118.629	-71.466	-77.604
Taiwan SMART1	Max	86.467	104.069	78.906	94.148
	Min	-124.619	-101.739	-61.471	-86.524
Imperial valley 06	Max	168.281	105.6	75.48	76.877
	Min	-155.765	-115.922	-85.992	-63.481
Imperial valley 02	Max	89.959	111.306	91.877	70.764
	Min	-108.858	-103.288	-109.889	-77.065

Table 8: Maximum roof displacements for 5-story structures

Earthquake Event		Vulnerable		Retrofitted	
		X Direction (mm)	Y Direction (mm)	X Direction (mm)	Y Direction (mm)
Northridge-01	Max	309.066	127.22	165.189	92.207
	Min	-226.44	-139.158	-202.145	-80.257
Cape Mendocino	Max	231.701	260.482	100.933	81.331
	Min	-222.777	-347.697	-90.76	-73.49
Spitak Armenia	Max	220.721	128.377	177.202	75.62
	Min	-165.451	-142.662	-176.746	-50.037
Superstition hills 02	Max	145.638	157.311	174.812	100.198
	Min	-203.61	-379.391	-162.33	-115.563
Taiwan SMART1	Max	195.22	147.897	166.247	101.351
	Min	-183.203	-116.262	-156.062	-143.688
Imperial valley 06	Max	162.259	195.763	159.274	266.083
	Min	-148.371	-193.071	-153.836	-221.647
Imperial valley 02	Max	160.248	168.379	107.859	106.96
	Min	-152.79	-197.488	-116.305	-117.858

Table 9: Maximum roof displacements for 7-story structures

Earthquake Event		Vulnerable		Retrofitted	
		X Direction (mm)	Y Direction (mm)	X Direction (mm)	Y Direction (mm)
Northridge-01	Max	398.247	175.502	346.078	146.161
	Min	-241.51	-203.32	-321.416	-139.029
Cape Mendocino	Max	322.732	295.613	76.411	110.687
	Min	-339.033	-448.524	-83.797	-105.776

Spitak Armenia	Max	284.581	138.983	287.335	153.666
	Min	-179.144	-158.563	-285.455	-156.144
Superstition hills 02	Max	220.628	224.927	152.974	214.875
	Min	-312.271	-493.042	-150.687	-220.215
Taiwan SMART1	Max	274.266	239.289	121.727	171.846
	Min	-237.875	-243.382	-140.971	-170.909
Imperial valley 06	Max	160.643	232.886	167.584	219.625
	Min	-172.28	-235.595	-158.045	-225.811
Imperial valley 02	Max	222.035	188.532	230.922	152.569
	Min	-217.361	-237.478	-247.042	-157.166

4.4.1.2 Roof Acceleration

Floor acceleration demands are typically one of the primary sources of damage to nonstructural components. Suspended ceilings, piping and ventilation systems, and electrical wiring are examples of nonstructural components sensitive to acceleration. Many facilities, such as hospitals, rely on the functionality of these components. Therefore, this section is dedicated to examining the absolute acceleration results obtained from the NTHA of both the vulnerable and retrofitted models.

Tables 10, 11, and 12 detail the absolute roof acceleration that emerged due to the induced seismic demands. In general, it was observed that the acceleration demands for the roofs in all retrofitted structures have increased compared with vulnerable buildings. This might be attributed to the overall increase in stiffness of these structures despite the increase in their masses. Figure 23-25 shows an example of roof acceleration obtained by the time-history analysis in the set of buildings under investigation in response to the "Imperial Vally-02" excitation. Although this is an alarming result and often considered an undesirable outcome, further investigation into

the interstory drift ratio will give the final verdict on the potential nonstructural damage that might occur.

Table 10: Maximum roof acceleration for 3-story structures

Earthquake Event		Vulnerable		Retrofitted	
		X Direction (mm/s ²)	Y Direction (mm/s ²)	X Direction (mm/s ²)	Y Direction (mm/s ²)
Northridge-01	Max	4963.62	8818.61	8869.48	6915.5
	Min	-5460.99	-8602.54	-9340.35	-6600.99
Cape Mendocino	Max	5855.67	6427.37	10140.25	14189.71
	Min	-5380.95	-7507.17	-10056.85	-10789.77
Spitak Armenia	Max	5769.92	8941.33	10214.74	13541.78
	Min	-5734.68	-7110.21	-10925.93	-12434.89
Superstition hills 02	Max	6692.42	7564.7	9530.78	11614.63
	Min	-7075.63	-7820.15	-10887.22	-12024.59
Taiwan SMART1	Max	8502.89	6694.99	9862.74	13184.7
	Min	-7366.43	-7130.41	-10662.73	-12631.22
Imperial valley 06	Max	10488.42	7957.28	12331.95	9478.76
	Min	-9426.58	-7449.77	-11763.84	-10598.8
Imperial valley 02	Max	7578.57	9212.15	16052.32	11377.18
	Min	-7052.63	-8352.16	-14556.24	-9541.39

Table 11: Maximum roof acceleration for 5-story structures

Earthquake Event		Vulnerable		Retrofitted	
		X Direction (mm/s ²)	Y Direction (mm/s ²)	X Direction (mm/s ²)	Y Direction (mm/s ²)
Northridge-01	Max	6076.05	3598.26	14465.02	7385.49
	Min	-7446.74	-3996.82	-11458.29	-8533.77
Cape Mendocino	Max	4656.59	6742.79	7317.05	5748.31
	Min	-6212.91	-7119.6	-8772.71	-7201.88
Spitak Armenia	Max	5230.85	7099.6	14157.63	7700.54
	Min	-6445.68	-6442.74	-12779.73	-7600.94
Superstition hills 02	Max	5223.59	6303.13	13377.55	8408.15
	Min	-3908.33	-3987.23	-13751.57	-7904.8
Taiwan SMART1	Max	6383.95	5423.12	11612.52	9628.09
	Min	-6120.47	-3829.24	-12383	-8581.42

Imperial valley 06	Max	5042.74	6570.77	11266.58	15875.95
	Min	-5691.91	-5824.19	-10899.98	-18322.65
Imperial valley 02	Max	7444.87	6874.23	12601.19	10211.09
	Min	-6488.93	-6395.32	-10774.62	-9643.28

Table 12: Maximum roof acceleration for 7-story structures

Earthquake Event		Vulnerable		Retrofitted	
		X Direction (mm/s ²)	Y Direction (mm/s ²)	X Direction (mm/s ²)	Y Direction (mm/s ²)
Northridge-01	Max	5697.59	4976.81	16502.52	12871.1
	Min	-7565.96	-4114.98	-18701.27	-12934.29
Cape Mendocino	Max	5842.39	7821.09	10526.89	8817.68
	Min	-5301.43	-6951.04	-11058.14	-6928.05
Spitak Armenia	Max	4411.33	8184.49	16083.47	12575.24
	Min	-6027.56	-6719.12	-13375.65	-16117.39
Superstition hills 02	Max	6222.39	7200.11	8394.76	12580.92
	Min	-5301.49	-4320.45	-8581.64	-11778.47
Taiwan SMART1	Max	5353.61	7318.86	7339.24	10874.37
	Min	-6150.42	-6738.89	-7388.96	-8246.79
Imperial valley 06	Max	6167.09	6424.07	9169.26	12365.17
	Min	-5599.26	-6533.91	-9765.32	-13357.39
Imperial valley 02	Max	5891.79	4762.47	16715.75	8878.96
	Min	-7771.46	-5079.28	-14248.24	-8708.5

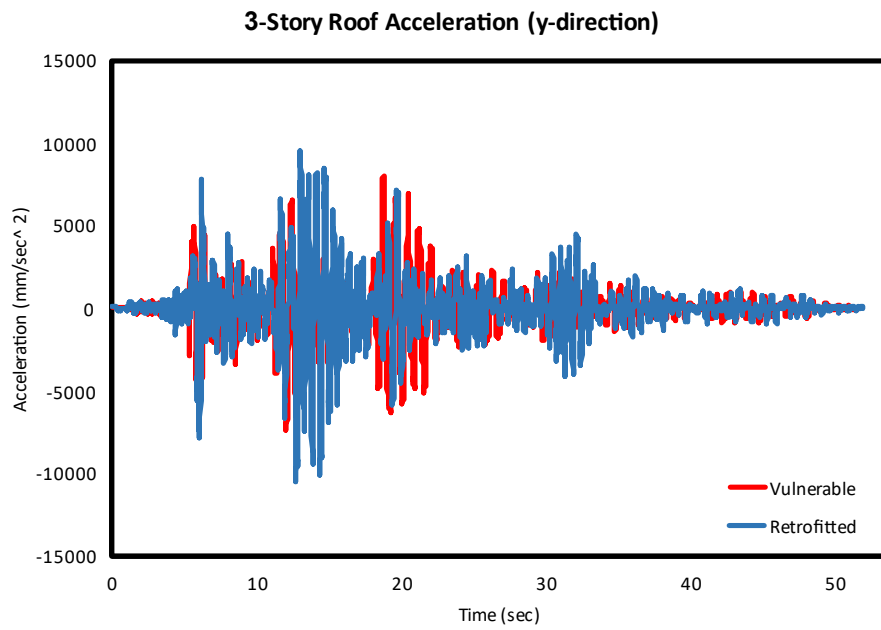
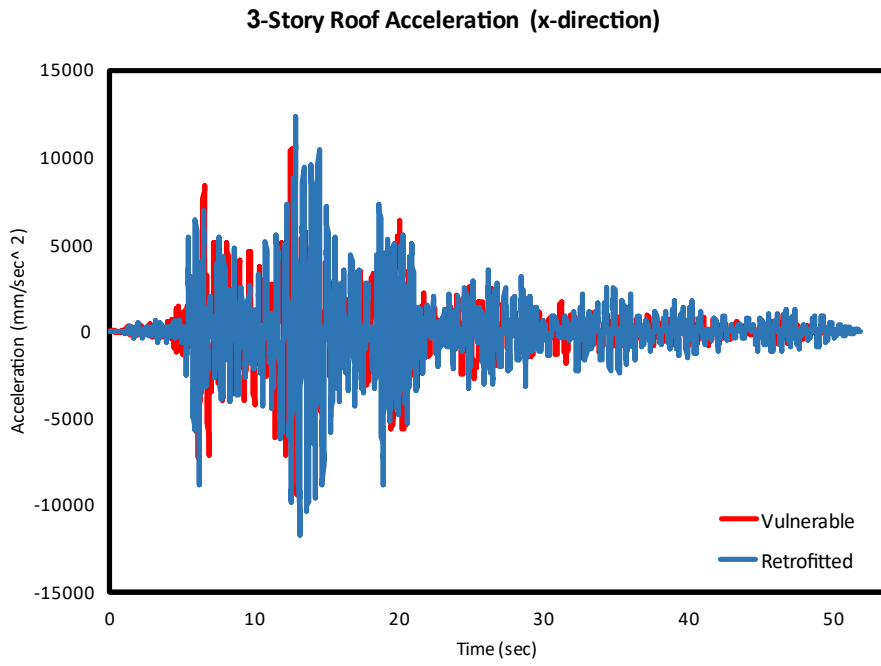


Figure 23: 3-story buildings' roof acceleration time history in response to "Imperial Valley-02" earthquake record

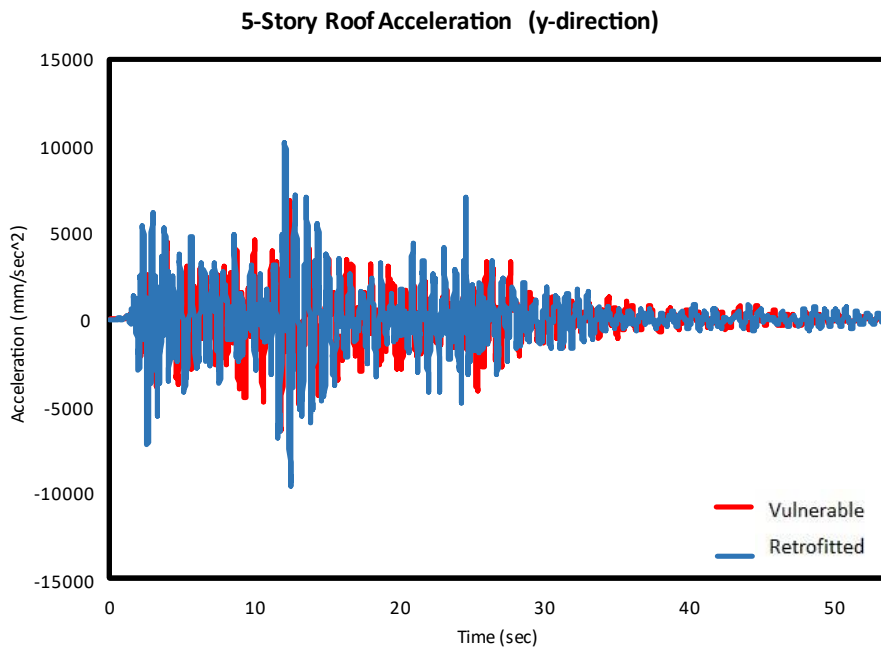
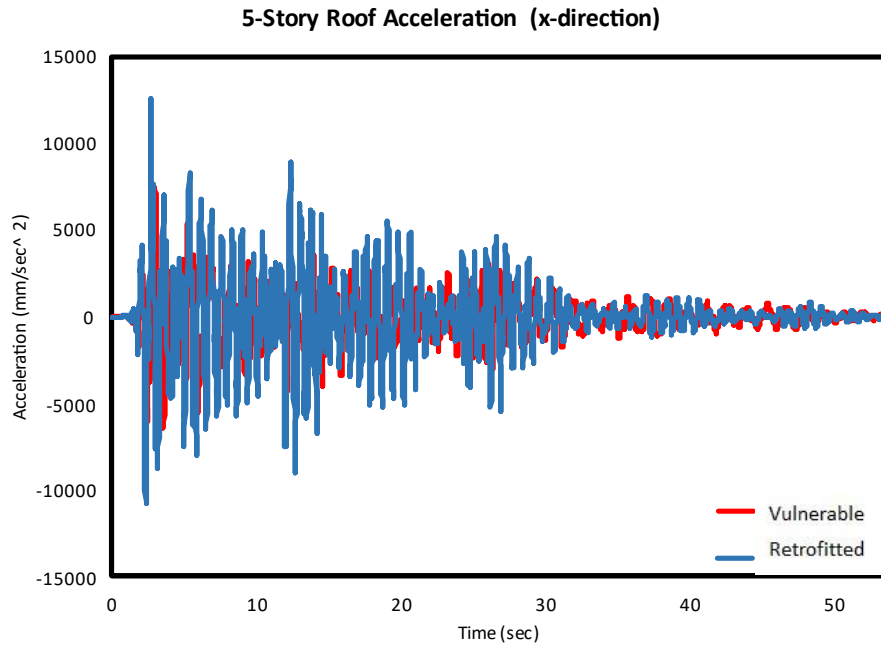


Figure 24: 5-story buildings' roof acceleration time history in response to "Imperial Valley-02" earthquake record

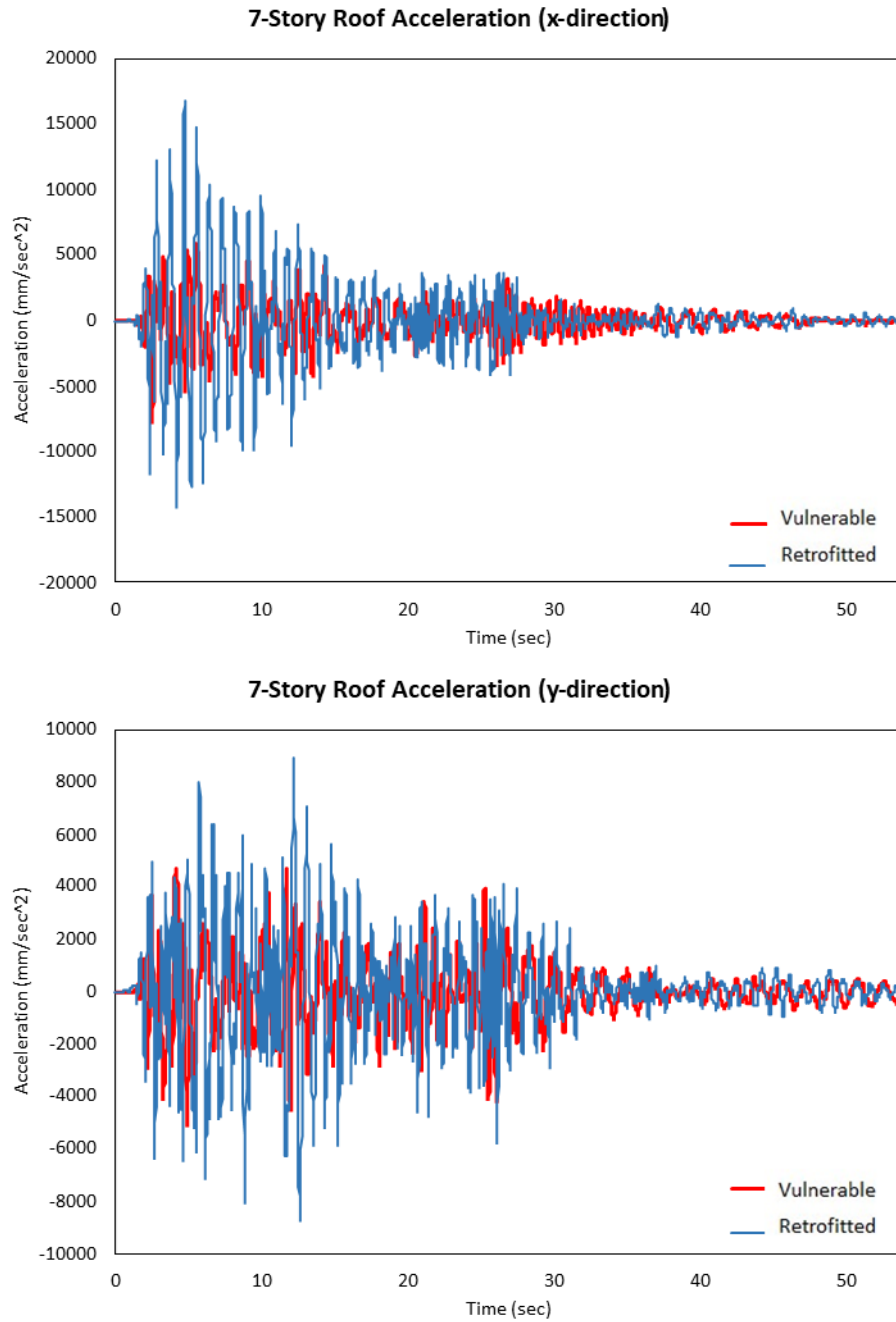


Figure 25: 7-story buildings' roof acceleration time history in response to "Imperial Valley-02" earthquake record

4.4.1.2 Interstory Drift Ratio

The seismic performance of buildings is often evaluated through the maximum interstory drift ratio (IDR) measured at each story level. IDR is considered a critical seismic parameter because it is directly related to the extent of lateral structural damage. This ratio is defined as the lateral story displacement obtained as the

difference between the top and bottom floor displacement normalized by the story's height. In this study, the maximum IDRs produced from the NTHA were compared to the suggested interstory drift values from Eurocodes associated with damage limitation both for structural and nonstructural components. EC8 suggests the limit of $\pm 2.5\%$ IDR for the typical moment-resisting frames where nonstructural elements do not interfere with the global structural response.

In Figures 26 and 27, it is seen that all the structural models, including the vulnerable ones, have generated maximum drifts within the allowable limits. However, the retrofitted structures exhibited smaller drift ratios, especially for the lower stories. For instance, the maximum IDR occurring in the vulnerable buildings was calculated as 0.022 (2.2%) when the model was subjected to "Imperial Valley-06" earthquake; this value was decreased to 0.0057 (0.57%) in the retrofitted model considering the same seismic record.

In 5-story models, the vulnerable structures suffered IDR that exceeds the limit of $\pm 2.5\%$. This can be seen in Figures 28 and 29, under the "Superstition Hill-02", "Northridge-01", and "Cape Mendocino" data. Improvements are evident in the data obtained from the retrofitted structures as their respective IDRs calculated are less than the allowable limit described in the codes.

Similarly, 7-story IDRs results showcase a similar trend to that highlighted in the 5-story models where the vulnerable buildings did not satisfy the performance objective, whereas the retrofitting helped rectify the deficiencies and produced IDRs within limits to ensure satisfactory seismic performance (Figures 30 and 31). One example can be the IDR in y-direction in response to "Superstition Hills-02" records, where the

calculated maximum IDR was reduced from -0.039 (-3.9%) to -0.012 (-1.2%) in the retrofitted model. It is noteworthy that the IDR data obtained from the nonlinear analysis eliminated any concerns raised upon the inspection of the roof acceleration results regarding the susceptibility of nonstructural components to damage in the retrofitted buildings.

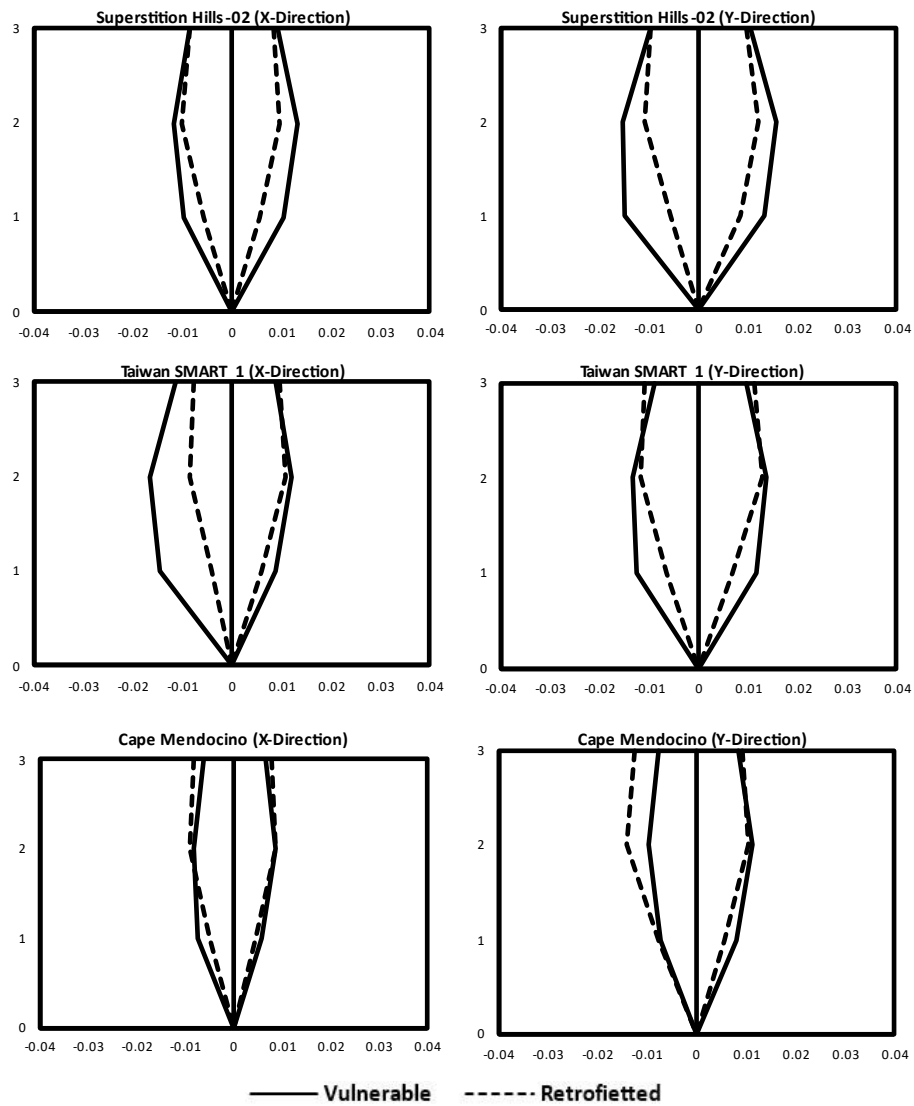


Figure 26: Interstory drift ratio for the 3-story models.

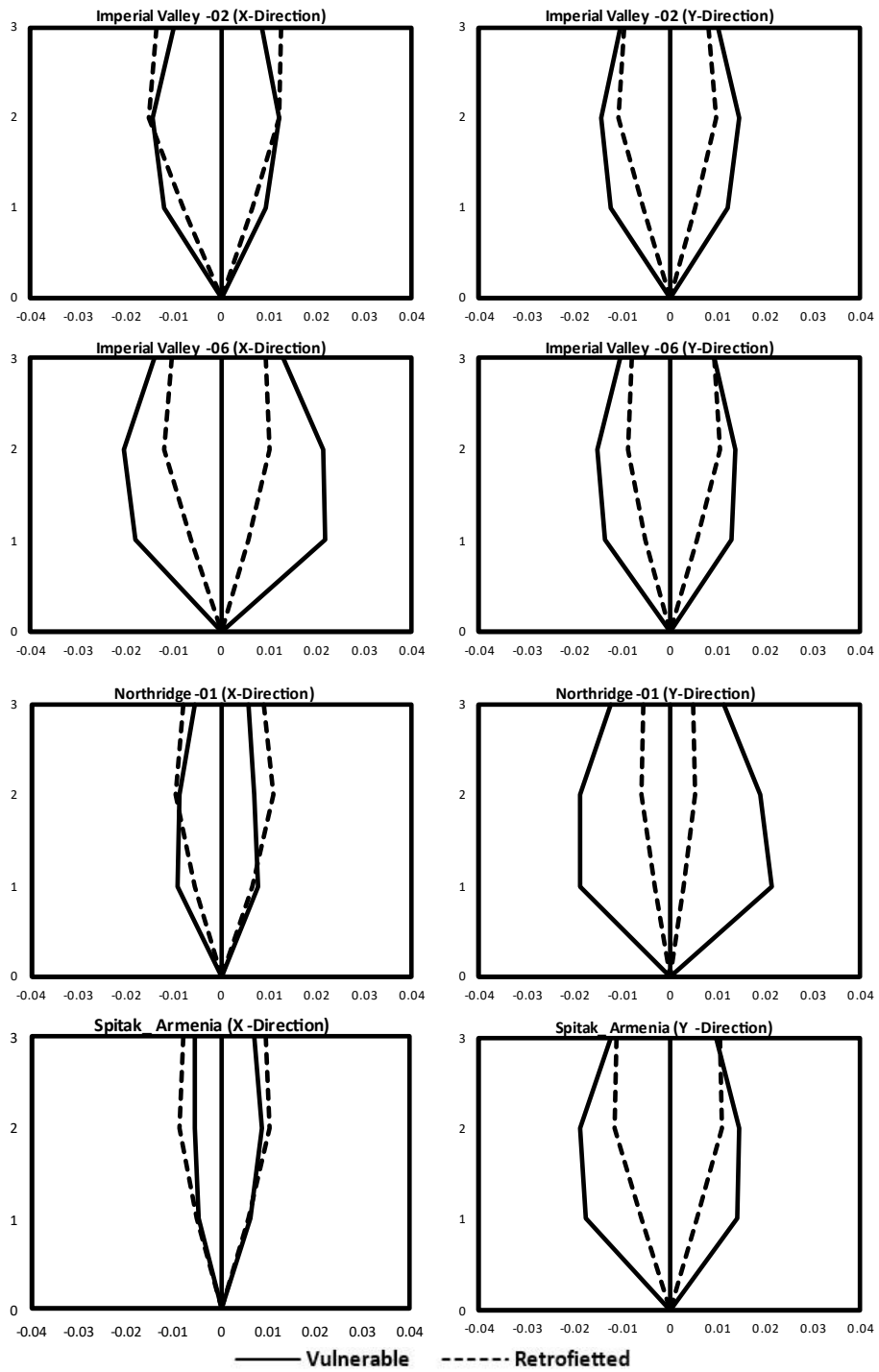


Figure 27: Interstory drift ratio for the 3-story models (continued).

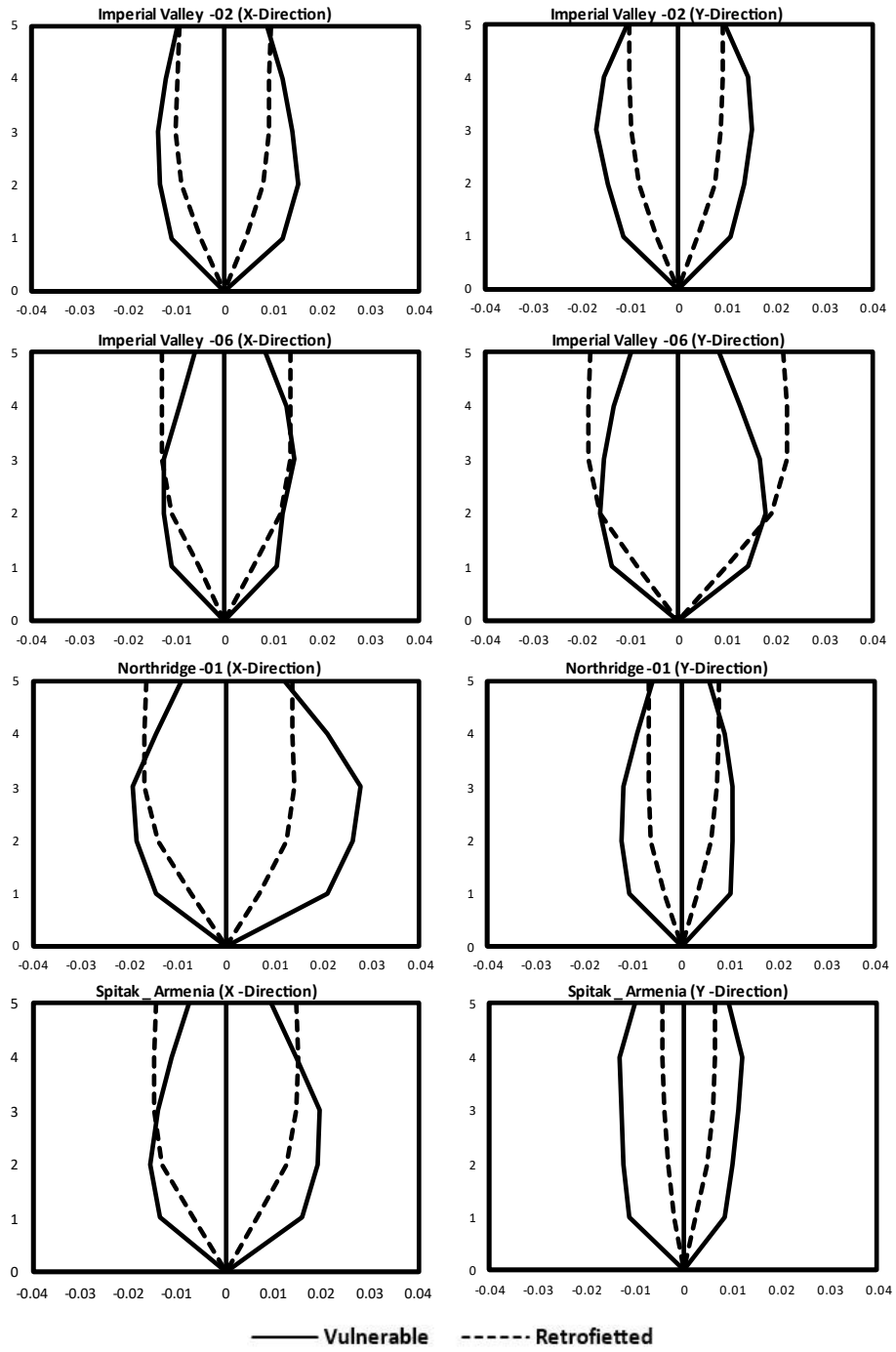


Figure 28: Interstory drift ratio for the 5-story models

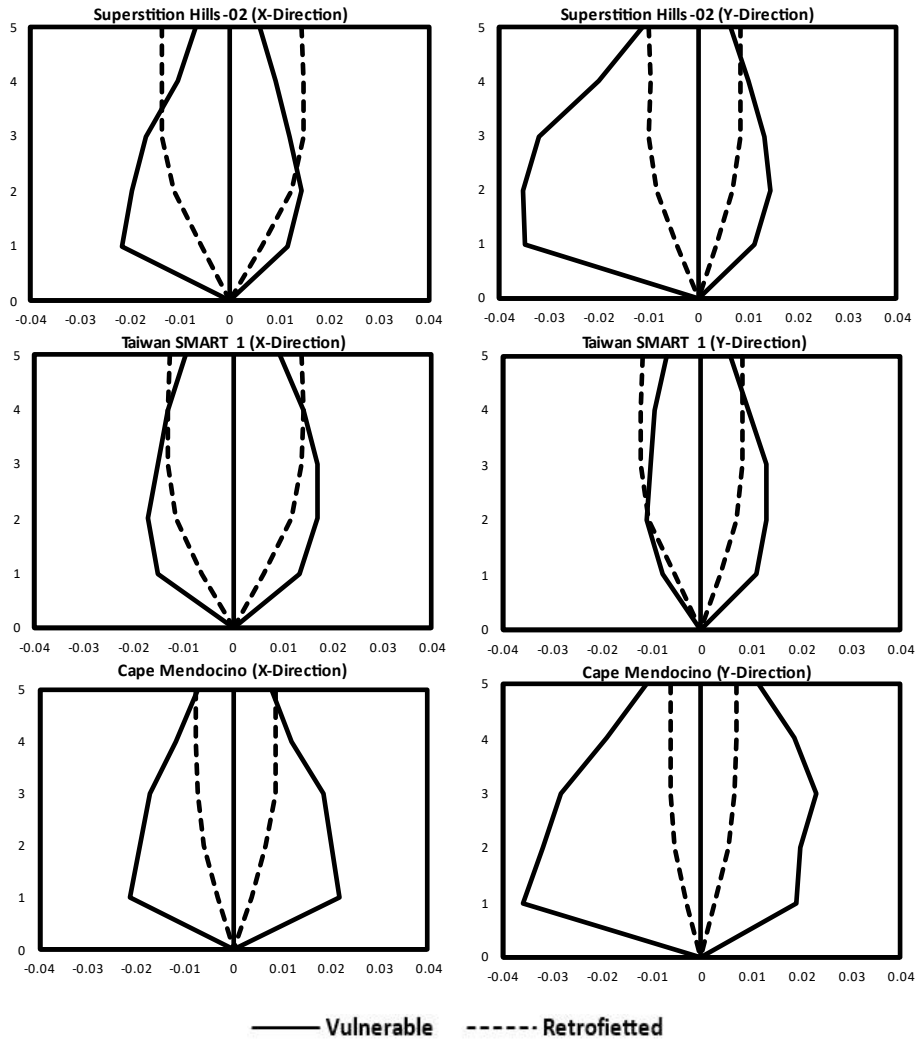


Figure 29: Interstory drift ratio for the 5-story models (continued)

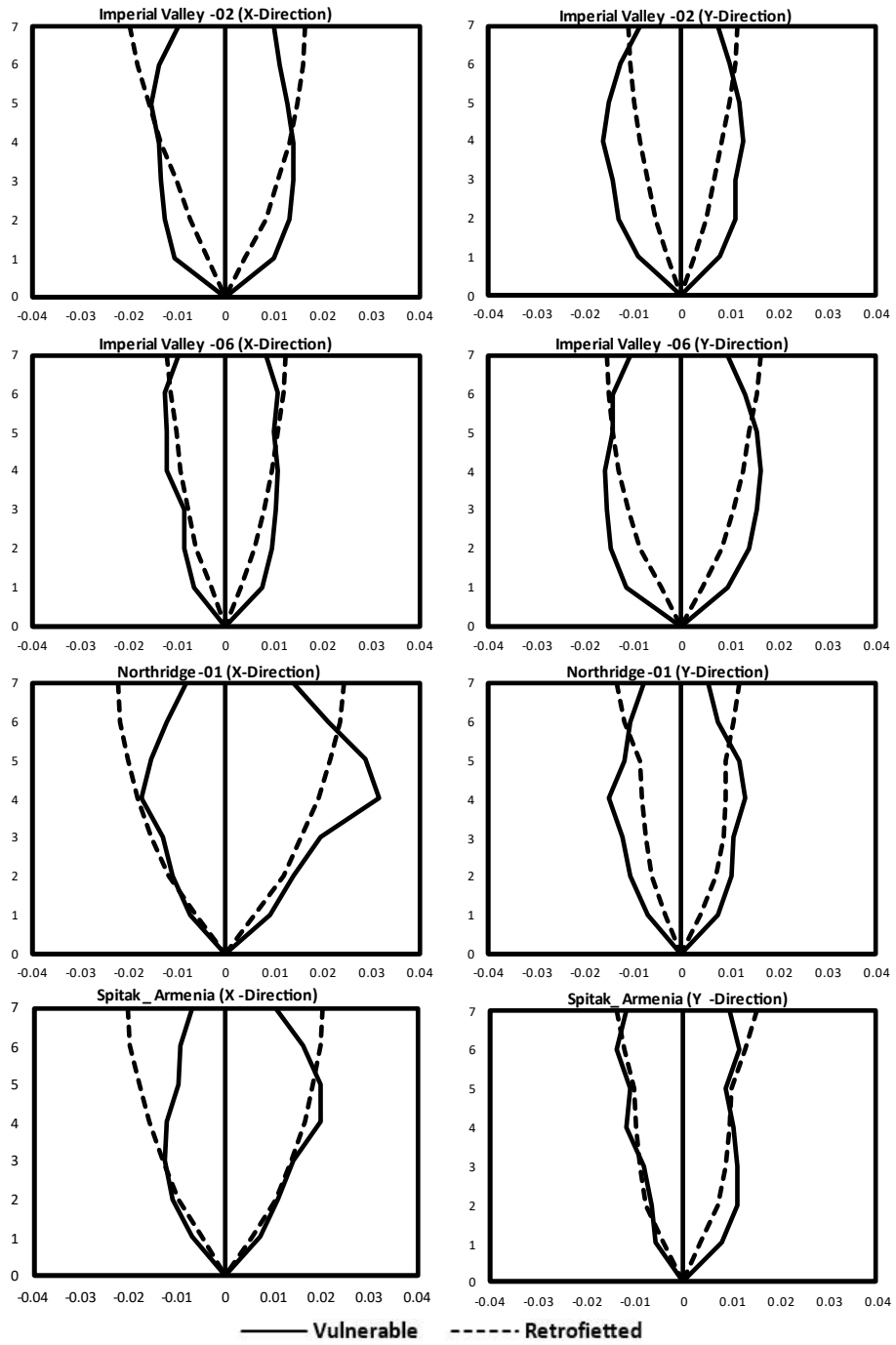


Figure 30: Interstory drift ratio for the 7-story models

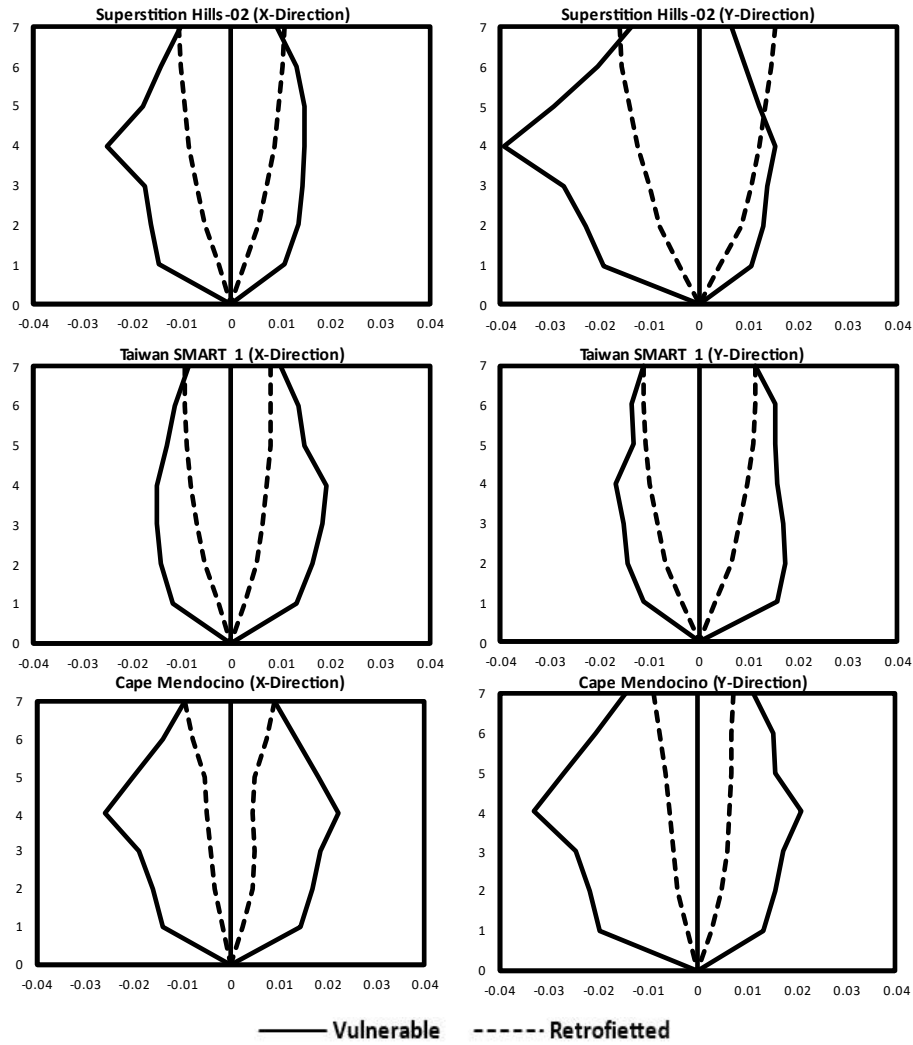


Figure 31: Interstory drift ratio for the 7-story models (continued)

4.4.1.2 Energy Components

Energy component assessment is another convenient tool available in ETABS to study the structural performance under seismic loading. Typically, the energy input induced by the earthquake is either dissipated through global damping or inelastic actions and deformations. When ground shaking occurs, causing permanent structural damage, the total input energy is divided between the stored potential and kinetic energies, dissipated damping energy, and the inelastic energy (also known as the hysteretic energy) released in the form of inelasticity.

For the purpose of this study, the energy-based method of assessment is demonstrated in detail for the most unfavorable earthquake scenario considered in terms of the number of failing members. For all bare structures, "Superstition Hills-02" created the most damage and failures compared to other earthquake records included in the analysis (which will be discussed in detail in the following section).

As depicted in Figures 32,33, and 34, the vulnerable structures suffered permanent damage in the form of hysteretic energy. Moreover, the lack of adequate ductility led to the inevitable failure of some of the structural members. The percentage of hysteretic energy to input energy ratio for the vulnerable buildings was found to be 22%, 46%, and 36% for the 3-story, 5-story, and 7-story, respectively. On the other hand, the retrofitted structures displayed a negligible ratio ($>1.5\%$ in all models) as the permanent damage endured was not significant and the structure behaved mostly within the elastic limit.

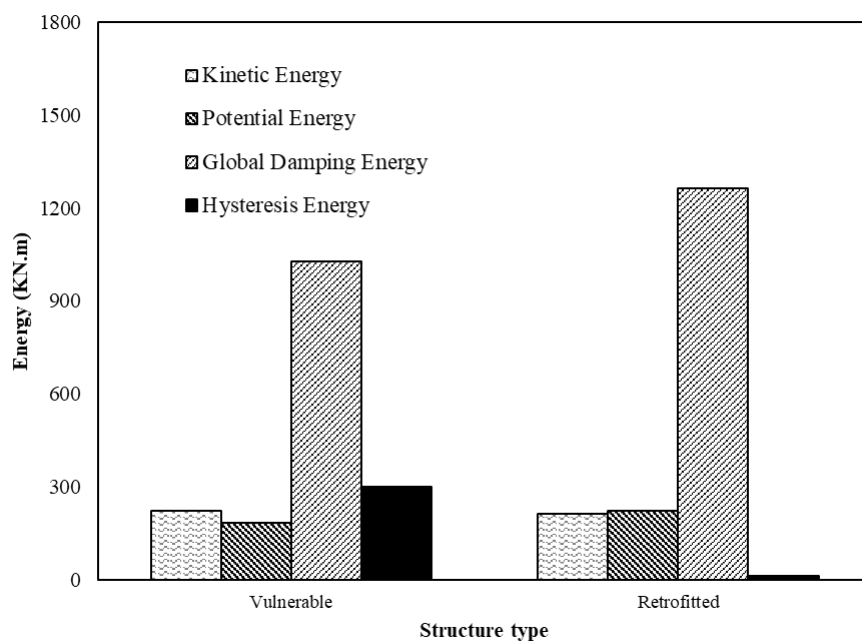


Figure 32: The total energy components encountered by the 3-story models under "Superstition Hills-02" seismic activity

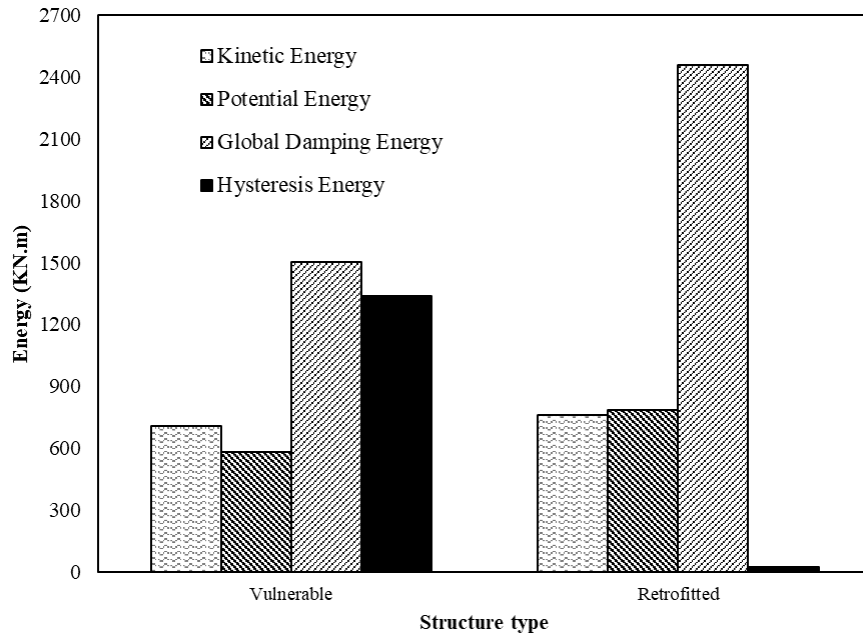


Figure 33: The total energy components encountered by the 5-story models under “Superstition Hills-02” seismic activity

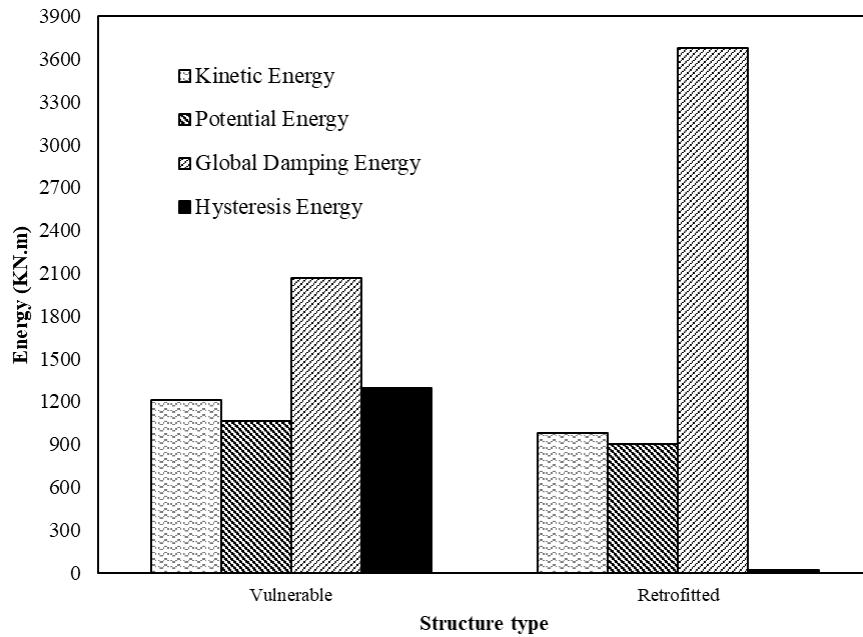


Figure 34: The total energy components encountered by the 7-story models under “Superstition Hills-02” seismic activity

4.4.2 Local Responses

This section will present the analysis result of the localized performance for each element within the buildings studied. All the observations will be made by tracking

the formation of nonlinear plastic hinges, defined at the ends of each frame element, during the excitation period from the different earthquake events considered in the NTHA. The performance levels (i.e., limit states) are classified depending on the impact of earthquakes and the damage state of the element into:

- Immediate Occupancy (IO): The element is only damaged lightly, without significant yielding.
- Life safety (LS): The structural element is damaged inelastically but still maintaining some residual lateral strength and stiffness.
- Collapse Prevention (CP): The structural element is damaged heavily, and incapable of surviving another earthquake.
- >CP: The element collapsed.

To begin with, the 3-story vulnerable buildings suffered localized failure at the base of the structure, similar to those shown in Figure 35, in response to the earthquake events considered in the nonlinear analysis. As seen in Table 13, a minimum of 14 out of 16 base columns failed under the seismic excitation in each individual earthquake event. In comparison, the retrofitting system succeeded in addressing the weakness of the vulnerable buildings, which is evident by the change in performance of failing members from >CP to IO in all of the cases evaluated.

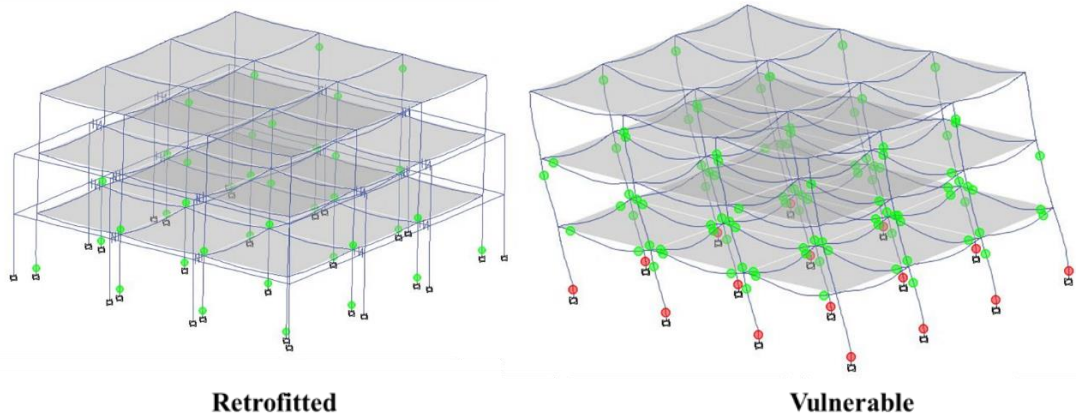


Figure 35: Hinge state at the end of Superstition hills 02 record for the 3-story models

As for the 5-story models, the seismic response of vulnerable structures to the selected suite of ground motion records was the most drastic given the number of plastic hinges formed compared to the total number of hinges defined in the model (Table 14). The number of hinges that failed ranged from 16, in the least devastating, to 85 in the most destructive earthquake case (Figure 36). The proposed retrofitting system proved its efficiency in this case as the post-earthquake limit state of the structural elements changed from total collapse ($>CP$) to IO in some events (Cape Mendocino, Superstition hills 02, Taiwan SMART1, Spitak Armenia, and Imperial valley 02) whereas it was reduced to LS in others (Northridge-01, and Imperial valley 06).

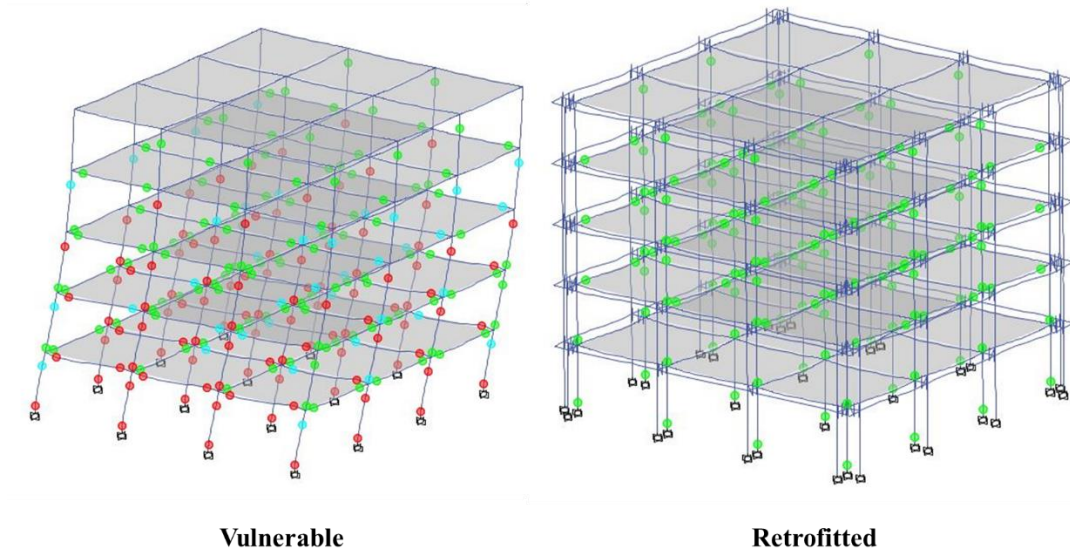


Figure 36: Hinge state at the end of Superstition hills 02 record for the 5-story models

Likewise, the same conclusion can be drawn from the state of hinges in the 7-story models. The results (Table 15) show that all the failing hinges formed in the vulnerable structures are subsided to IO (Cape Mendocino, Superstition hills 02, Taiwan SMART1, and Imperial valley 02) and LS performance levels (Northridge-01, Spitak Armenia, and Imperial valley 06) in the analysis, meaning that the structure remains safe to occupy after the earthquake event since it retains most of the pre-earthquake strength and stiffness.

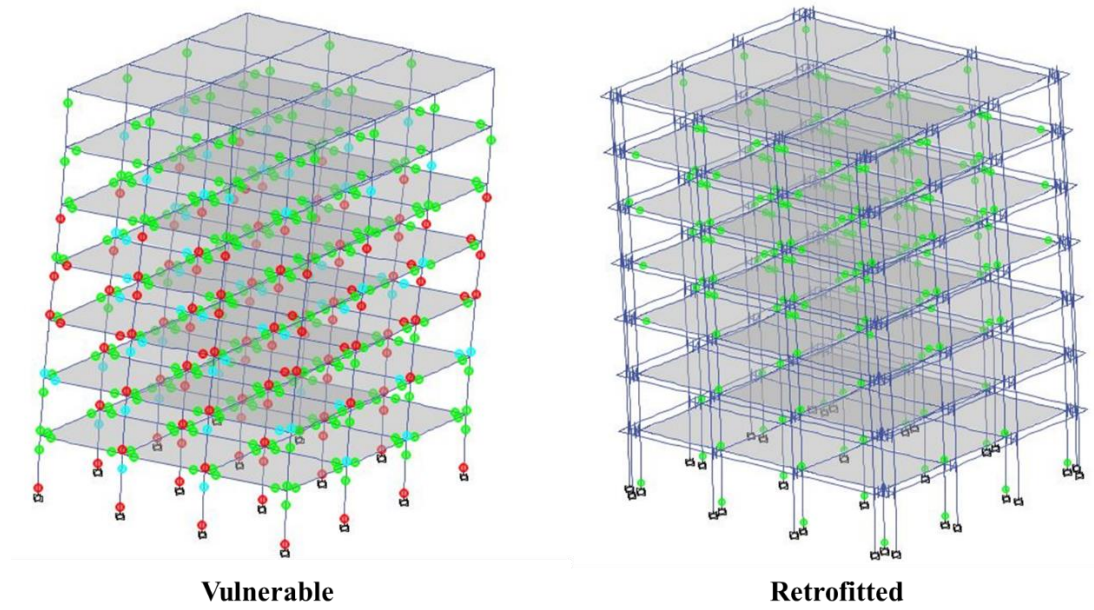


Figure 37: Hinge state at the end of Superstition hills 02 record for the 7-story models

Table 13: State of hinges in 3-story models

Earthquake Event	Structure Type	Total Number of Hinges	Plastic Hinges					
			Beam			Column		
			IO	LS	CP	IO	LS	>CP
Northridge-01	Vulnerable	240	48	0	0	38	16	16
	Retrofitted	336	0	0	0	15	0	0
Cape Mendocino	Vulnerable	240	0	0	0	30	10	0
	Retrofitted	336	9	0	0	42	0	0
Spitak Armenia	Vulnerable	240	46	0	0	44	0	16
	Retrofitted	336	0	0	0	35	0	0
Superstition hills 02	Vulnerable	240	48	0	0	52	0	16
	Retrofitted	336	0	0	0	38	0	0
Taiwan SMART1	Vulnerable	240	61	0	0	50	2	14
	Retrofitted	336	2	0	0	52	0	0
Imperial valley 06	Vulnerable	240	77	3	0	43	14	16
	Retrofitted	336	0	0	0	43	0	0
Imperial valley 02	Vulnerable	240	50	0	0	48	1	15
	Retrofitted	336	14	0	0	45	0	0

Table 14: State of hinges in 5-story models

Earthquake Event	Structure Type	Total Number of Hinges	Plastic Hinges					
			Beam			Column		
			IO	LS	>CP	IO	LS	>CP
Northridge-01	Vulnerable	400	90	23	4	49	26	52
	Retrofitted	760	71	0	0	105	4	0
Cape Mendocino	Vulnerable	400	125	21	22	31	29	73
	Retrofitted	760	0	0	0	0	0	0
Spitak Armenia	Vulnerable	400	127	0	0	84	24	16
	Retrofitted	760	74	0	0	77	0	0
Superstition hills 02	Vulnerable	400	95	19	26	25	21	85
	Retrofitted	760	70	0	0	98	0	0
Taiwan SMART1	Vulnerable	400	127	0	0	85	0	16
	Retrofitted	760	74	0	0	81	0	0
Imperial valley 06	Vulnerable	400	144	0	0	92	20	16
	Retrofitted	760	147	2	0	84	40	0
Imperial valley 02	Vulnerable	400	168	0	0	97	4	16
	Retrofitted	760	0	0	0	42	0	0

Table 15: State of hinges in 7-story models

Earthquake Event	Structure Type	Total Number of Hinges	Plastic Hinges					
			Beam			Column		
			IO	LS	>CP	IO	LS	>CP
Northridge-01	Vulnerable	560	167	4	6	78	37	55
	Retrofitted	1064	136	0	0	141	35	0
Cape Mendocino	Vulnerable	560	239	19	6	73	40	83
	Retrofitted	1064	0	0	0	23	0	0
Spitak Armenia	Vulnerable	560	132	0	0	123	39	15
	Retrofitted	1064	132	0	0	133	23	0
Superstition hills 02	Vulnerable	560	225	27	13	46	41	109
	Retrofitted	1064	81	0	0	116	0	0
Taiwan SMART1	Vulnerable	560	247	0	0	113	51	32
	Retrofitted	1064	0	0	0	54	0	0
Imperial valley 06	Vulnerable	560	130	0	0	133	38	16
	Retrofitted	1064	89	0	0	129	3	0
Imperial valley 02	Vulnerable	560	225	0	0	149	12	16
	Retrofitted	1064	90	0	0	117	0	0

4.5 Added Weight

It stands to reason that the encasement peripheral frame increases the overall weight of the retrofitted building. However, the existing building will not bear any of the additional weight as the retrofitting systems will have their own path to transmit the gravitational loads of the peripheral frame to the ground. To quantify the increase in weight, calculation shown in Table 16 has been performed to express the added concrete as a percentage of the total weight of bare structures. From the results obtained, it is clear that the added weight of the retrofitting system is a function of the vulnerable structures' height, where the additional weight increases exponentially with the increase in the number of stories. Moreover, it is worth mentioning that most of the additional weight is due to the wide peripheral columns, as they are the primary structural element providing rigidity and stiffness to the retrofitted building.

Table 16: Weight of structural elements for both vulnerable and retrofitted structures

Number of stories	Bare		Retrofitted		% Increase
	Object Type	Weight (KN)	Object Type	Weight (KN)	
3	Column	575.8299	Column	581.8281	15.86
	Beam	1117.47	Beam	88.4739	
	Floor	2530.5025			
	Total	4223.8024	Total	670.302	
5	Column	1009.202	Column	2549.247	41.6
	Beam	1858.401	Beam	398.0893	
	Floor	4217.5042			
	Total	7085.1072	Total	2947.333	
7	Column	1496.5579	Column	3790.889	64.5
	Beam	2677.1592	Beam	2744.958	
	Floor	5904.5089			
	Total	10078.226	Total	6505.847	

Chapter 5

CONCLUSION AND RECOMMENDATION

5.1 Conclusion

This research sought to evaluate the seismic performance of a non-destructive retrofitting technique as a method for strengthening seismically deficient multi-story reinforced concrete moment-frame structures. The proposed system, namely the peripheral encasement technique, relies on confining the existing vulnerable building with stiff, reinforced concrete frames to address the structural deficiencies developed under seismic excitation. To make the study more comprehensive, low, mid, and high-rise buildings were investigated under a suite of diverse ground motion records representing the potential seismic hazard at the site of interest. The selected multistory RC structures have been first designed utilizing the linear static (Equivalent Lateral Force) method of analysis per Eurocode provisions and then weakened such that the structures are deemed vulnerable under seismic actions. After that, a performance-based analysis was conducted employing a series of Nonlinear Dynamic Time-History analyses on the vulnerable and retrofitted buildings in order to verify and evaluate the efficiency of the proposed strengthening system. The findings of the study can be summarized as follows:

- The results of the 3-story model showed that the newly designed buildings following the prescriptive code-based procedure that relies solely on linear analysis methods are still susceptible to damage under seismic excitations despite the inclusion of an equivalent lateral force in the design. Hence, the

current linear design provisions are not sufficient to ensure the safety of newly built structures in highly seismogenic regions.

- The natural vibration period of the retrofitted buildings was reduced significantly, attributed to the enhanced global stiffness provided by the peripheral frames. This was more prominent in mid and high-rise structures.
- In general, the retrofitted system immensely reduced the maximum roof displacement in both orthogonal directions (i.e., x and y). However, in some scenarios, the retrofitted structures experienced an increase in roof displacement but without endangering the structural elements or causing permanent damage. This indicates that the retrofitted structures' natural frequency might be closer to resonance with the considered ground motion records in these instances.
- The roof accelerations were observed to be higher in the retrofitted structures since the global structural stiffness increased upon incorporating the peripheral frames. However, this higher acceleration was not sustained for a long period of time, unlike vulnerable buildings. This phenomenon is speculated to be directly linked with the decreased natural frequencies of the retrofitted structures.
- The inter-story drift ratios of the vulnerable structures indeed exceeded the allowable limits suggested by the Eurocodes, particularly for the mid and high-rise buildings. This is unwelcomed since it might cause damage to the nonstructural elements. On the other hand, retrofitted structures remained below the allowable limits by a large margin regardless of the intensity of the ground motion record or the height of the building.

- The hysteretic to input energy ratio was significantly higher for the vulnerable buildings compared with the retrofitted structures. This increase in the hysteretic energy indicates permanent damage or sometimes even failure within the structure. On the contrary, the retrofitted structures encountered negligible hysteretic energy where the seismically induced energy input was dissipated mainly in the form of global damping energy.
- The vulnerable bare structures developed many plastic hinges with Collapse Prevention or Complete Collapse limit state. The formation of such hinges was observed in the vulnerable structures, particularly in ground floor columns, which threatens the global integrity of these structures. This was the common trend in response to all of the earthquake records analyzed. On the contrary, the retrofitted structures' hinges were predominantly Immediate occupancy, although some Life Safety hinges are developed for mid and high-rise structures. Nevertheless, this will not jeopardize the safety of the occupants or menace the functionality of the structures.

To sum up, the proposed retrofitting technique proved its capability to rehabilitate existing seismically weak structures as it showed satisfactory performance, notably in the case of retrofitting a low-rise building.

5.2 Recommendations

This research covered the evaluation of a proposed encasement technique to strengthen vulnerable reinforced concrete structures. However, some aspects were not investigated in the study and can be suggested for future research work. These aspects are discussed below.

- Soil-structure interaction was not considered in this research, which might play a significant role in the overall behavior of the retrofitted system as two shallow foundations will be situated in the same vicinity.
- The influence of plan and elevation irregularities was not within the study's scope, and this influence can severely impact the structure's seismic performance.
- This research focused on axial and flexural failures as the shear failures were implicitly accounted for by the fiber hinges used in the nonlinear analysis. Therefore, detailed examination of the shear failures that might take place is highly recommended.
- The numerical simulation findings of the proposed retrofitting technique should be verified with experimental work.
- A larger suite of earthquakes containing diverse earthquake data and different soil classes should be considered in the nonlinear analysis to ensure the efficiency of the retrofitting system against various seismic hazards.
- In future studies, the use of different analysis software is recommended to validate the results.

REFERENCES

- ACI Committee. (2002). Building code requirements for structural concrete:(ACI 318-02) and commentary (ACI 318R-02). *American Concrete Institute*.
- Alam, M. S., Nehdi, M., & Youssef, M. A. (2009). Seismic performance of concrete frame structures reinforced with superelastic shape memory alloys. *Smart Struct Syst*, 5(5), 565-585.
- Ali, Q. (2009). Seismic Retrofitting and Repair Manual for Buildings. *National Disaster*.
- Ambrose, J., & Vergun, D. (1999). *Design for earthquakes*. John Wiley & Sons.
- Arlekar, J. N., Jain, S. K., & Murty, C. V. R. (1997, November). Seismic response of RC frame buildings with soft first storeys. In *Proceedings of the CBRI Golden Jubilee Conference on Natural Hazards in Urban Habitat* (pp. 10-11).
- Basnet, R. (2021). Vertical Irregularity Effect on Fundamental Time Period and Critical Columns of Building Structures. (Doctoral dissertation, Southern Illinois University at Carbondale).
- Berry, M. P., & Eberhard, M. O. (2008). Performance Modeling Strategies for Modern Reinforced Concrete Bridge. *University of California, Berkeley*.

- Bouvier, C. A. (2003). *Techniques of seismic retrofitting for concrete structures* (Doctoral dissertation, Massachusetts Institute of Technology).
- Bruno, S., & Valente, C. (2002). Comparative response analysis of conventional and innovative seismic protection strategies. *Earthquake engineering & structural dynamics*, *31*(5), 1067-1092.
- Campione, G., Fossetti, M., Giacchino, C., & Minafò, G. (2014). RC columns externally strengthened with RC jackets. *Materials and Structures/Materiaux et Constructions*, *47*(10), 1715-1728.
- Cao, X. Y., Wu, G., Feng, D. C., & Zu, X. J. (2019). Experimental and numerical study of outside strengthening with precast bolt-connected steel plate-reinforced concrete frame-brace. *Journal of Performance of Constructed Facilities*, *33*(6), 04019077.
- Cao, X. Y., Wu, G., Feng, D. C., Wang, Z., & Cui, H. R. (2020). Research on the seismic retrofitting performance of RC frames using SC-PBSPC BRBF substructures. *Earthquake Engineering & Structural Dynamics*, *49*(8), 794-816.
- Chandrakar, J., & Singh, A. K. (2017). Study of Various Local and Global Seismic Retrofitting Strategies—A review. *Int. J. Eng. Res. Technol*, *6*, 824-831.
- Cheung, M., Foo, S., & Granadino, J. (2000). Seismic retrofitting of existing buildings: innovative alternatives. In *International Conference on the Seismic Performance of Traditional Buildings, Istanbul, Turkey, November* (pp. 16-18).

- Constantinou, M. C., & Symans, M. D. (1993). Seismic response of structures with supplemental damping. *The Structural Design of Tall Buildings*, 2(2), 77-92.
- CSI. (2019). ETABS Integrated Analysis, Design and Drafting of Building Systems. California: Computers and Structures Inc.
- De Luca, A., & Guidi, L. G. (2019). State of art in the worldwide evolution of base isolation design. *Soil Dynamics and Earthquake Engineering*, 125, 105722.
- Dusicka, P., & Tinker, J. (2013). Global restraint in ultra-lightweight buckling-restrained braces. *Journal of Composites for Construction*, 17(1), 139-150.
- Elbahy, Y. I., Youssef, M. A., & Meshaly, M. (2019). Seismic performance of reinforced concrete frames retrofitted using external superelastic shape memory alloy bars. *Bulletin of Earthquake Engineering*, 17(2), 781-802.
- EN 1990 (2002). Eurocode 0—Basis of structural design, *European Committee for Standardization, rue de Stassart, 36, B-1050 Brussels*.
- EN 1991-1-1. (2002). Eurocode 1— Actions on structures – Part 1-1: General actions - Densities, self-weight, imposed loads for buildings, *European Committee for Standardization, rue de Stassart, 36, B-1050 Brussels*.
- EN 1992-1-1. (2004). Eurocode 2— Design of concrete structures – Part 1-1: General rules and rules for buildings, *European Committee for Standardization, rue de Stassart, 36, B-1050 Brussels*.

- EN 1998-1. (2004). Eurocode 8—Design of structures for earthquake resistance – Part 1: General rules, seismic actions and rules for buildings, *European Committee for Standardization, rue de Stassart, 36, B-1050 Brussels.*
- Ferraioli, M., & Avossa, A. M. (2012). Base isolation seismic retrofit of a hospital building in Italy. *Journal of Civil Engineering and Architecture, 6(3), 308.*
- Frosch, R. J., Li, W., Jirsa, J. O., & Kreger, M. E. (1996). Retrofit of non-ductile moment-resisting frames using precast infill wall panels. *Earthquake Spectra, 12(4), 741-760.*
- Habibi, A., Chan, R. W., & Albermani, F. (2013). Energy-based design method for seismic retrofitting with passive energy dissipation systems. *Engineering Structures, 46, 77-86.*
- Hertanto, E. (2005). Seismic assessment of pre-1970s reinforced concrete structure.
- Ilki, A., Demir, C., Bedirhanoglu, I., & Kumbasar, N. (2009). Seismic retrofit of brittle and low strength RC columns using fiber reinforced polymer and cementitious composites. *Advances in Structural Engineering, 12(3), 325-347.*
- Iwata, M., & Murai, M. (2006). Buckling-restrained brace using steel mortar planks; performance evaluation as a hysteretic damper. *Earthquake engineering & structural dynamics, 35(14), 1807-1826.*

- Kaliyaperumal, G., & Sengupta, A. K. (2009). Seismic retrofit of columns in buildings for flexure using concrete jacket. *ISET Journal of Earthquake Technology*, 46(2), 77-107.
- Kaplan, H., Yilmaz, S., Cetinkaya, N., & Atimtay, E. (2011). Seismic strengthening of RC structures with exterior shear walls. *Sadhana*, 36(1), 17-34.
- Kwon, J. (2016). *Strength, stiffness, and damage of reinforced concrete buildings subjected to seismic motions* (Doctoral dissertation).
- Maheri, M. R., & Ghaffarzadeh, H. (2008). Connection overstrength in steel-braced RC frames. *Engineering Structures*, 30(7), 1938-1948.
- Mander, J. B., Priestley, M. J., & Park, R. (1988). Theoretical stress-strain model for confined concrete. *Journal of structural engineering*, 114(8), 1804-1826.
- Masri, A. C., & Goel, S. C. (1996). Seismic design and testing of an RC slab-column frame strengthened by steel bracing. *Earthquake Spectra*, 12(4), 645-666.
- Michaud, D., & Léger, P. (2014). Ground motions selection and scaling for nonlinear dynamic analysis of structures located in Eastern North America. *Canadian journal of civil engineering*, 41(3), 232-244.
- Minafò, G. (2015). A practical approach for the strength evaluation of RC columns reinforced with RC jackets. *Engineering Structures*, 85, 162-169.

- Moehle, J. P. (2000). State of research on seismic retrofit of concrete building structures in the US. *Proceedings of US-Japan Symposium on Seismic Rehabilitation of Concrete Structures-State of Research and Practice-*.
- Naeim, F., & Kelly, J. M. (1999). *Design of seismic isolated structures: from theory to practice*. John Wiley & Sons.
- Navya, G., & Agarwal, P. (2016). Seismic retrofitting of structures by steel bracings. *Procedia Engineering*, 144, 1364-1372.
- NIST. (2017). Guidelines for Nonlinear Structural Analysis for Design of Buildings Part IIB-Reinforced Concrete Moment Frames. *National Institute of Standards and Technology*.
- Ortega, J., Vasconcelos, G., Rodrigues, H., Correia, M., Ferreira, T. M., & Vicente, R. (2019). Use of post-earthquake damage data to calibrate, validate and compare two seismic vulnerability assessment methods for vernacular architecture. *International journal of disaster risk reduction*, 39, 101242.
- Pampanin, S., Calvi, G. M., & Moratti, M. (2002). Seismic behavior of RC beam-column joints designed for gravity only.
- Park, R., & Paulay, T. (1991). *Reinforced concrete structures*. John Wiley & Sons.
- Pincheira, J. A., & Jirsa, J. O. (1995). Seismic response of RC frames retrofitted with steel braces or walls. *Journal of Structural Engineering*, 121(8), 1225-1235.

- Rizzo, A. R. (1991). FEA gap elements: Choosing the right stiffness. *Mechanical Engineering*, 113(6), 57.
- Rodriguez, M., & Park, R. (1991). Repair and strengthening of reinforced concrete buildings for seismic resistance. *Earthquake Spectra*, 7(3), 439-459.
- Safarizki, H. A., Kristiawan, S. A., & Basuki, A. (2013). Evaluation of the use of steel bracing to improve seismic performance of reinforced concrete building. *Procedia Engineering*, 54, 447-456.
- Solomos, G., Pinto, A., & Dimova, S. (2008). A review of the seismic hazard zonation in national building codes in the context of eurocode 8. *JRC Scientific and Technical reports*.
- Soong, T. T., & Spencer Jr, B. F. (2002). Supplemental energy dissipation: state-of-the-art and state-of-the-practice. *Engineering structures*, 24(3), 243-259.
- Sorace, S., & Terenzi, G. (2014). A viable base isolation strategy for the advanced seismic retrofit of an R/C building. *Contemp Eng Sci*, 7(17-20), 817-834.
- Symans, M. D., Charney, F. A., Whittaker, A. S., Constantinou, M. C., Kircher, C. A., Johnson, M. W., & McNamara, R. J. (2008). Energy dissipation systems for seismic applications: current practice and recent developments. *Journal of structural engineering*, 134(1), 3-21.

- Tena-Colunga, A., Del Valle, E., & Pérez-Moreno, D. (1996). Issues on the seismic retrofit of a building near resonant response and structural pounding. *Earthquake spectra*, 12(3), 567-597.
- Usami, T., Wang, C. L., & Funayama, J. (2012). Developing high-performance aluminum alloy buckling-restrained braces based on series of low-cycle fatigue tests. *Earthquake Engineering & Structural Dynamics*, 41(4), 643-661.
- Varadharajan, S., Sehgal, V. K., & Saini, B. (2014). Seismic response of multistory reinforced concrete frame with vertical mass and stiffness irregularities. *The structural design of tall and special buildings*, 23(5), 362-389.
- Xie, Q. (2005). State of the art of buckling-restrained braces in Asia. *Journal of constructional steel research*, 61(6), 727-748.
- Yakut, A. (2004). Reinforced concrete frame construction. *World Housing Encyclopedia—Summary Publication*.
- Youssef, M. A., & Elfeki, M. A. (2012). Seismic performance of concrete frames reinforced with superelastic shape memory alloys. *Smart Structures and Systems*, 9(4), 313-333.
- Youssef, M. A., Ghaffarzadeh, H., & Nehdi, M. (2007). Seismic performance of RC frames with concentric internal steel bracing. *Engineering Structures*, 29(7), 1561-1568.